Russian Chemical Reviews **76** (1) 59 – 78 (2007) © 2007 Russian Academy of Sciences and Turpion Ltd

DOI 10.1070/RC2007v076n01ABEH003629

Methods for investigation of the free volume in polymers

Yu P Yampolskii

Contents

I.	Introduction	59
II.	Positron annihilation lifetime spectroscopy	60
III.	^{129}Xe NMR spectroscopy	64
IV.	Inverse gas chromatography	65
V.	Miscellaneous methods	67
VI.	Simulation of the free volume by molecular dynamics	68
VII.	Conclusion	72
VIII.	Appendix	73

Abstract. Experimental probe methods for investigation of the free volume in polymers (positron annihilation lifetime spectroscopy, ^{129}Xe NMR spectroscopy and inverse gas chromatography) and relevant theoretical approaches (computer simulation) are considered. Various definitions of the free volume and related terms are given. The physical principles that underlie particular probe methods as well as the scope and limitations of each method are discussed. A systematic comparison of the size of free-volume elements in polymers determined by different methods is carried out. The bibliography includes 175 references.

I. Introduction

The notion of the free volume is of paramount importance for physical chemistry of polymers. Being initially formulated for liquid state,[1] it was extended to amorphous polymers that are either above or below the glass transition temperature (T_g).[2–5] The free volume in polymers determines their viscosity, relaxation and mechanical properties (deformation), thermal expansion, as well as the rates of interdiffusion of polymers and diffusion of low-molecular-mass species (gases and vapours) in polymers. Considering the free volume in polymers, one should keep in mind that this is not only an abstract physical parameter (although it can of course be described quantitatively), but also a real physical object characterised by an average size and shape of the 'hole' (a free-volume element, FVE), FVE size distribution, topology and connectivity (closed or open internal porosity). The FVE in glassy polymers are treated as 'frozen' in the polymer matrix. For rubbers, where the free volume has a fluctuation nature like in liquids, both the size of randomly formed FVE and the rate of their diffusion in the polymer matrix are essential.

The early phenomenological models treated the free volume as an abstract notion not related to the chemical structure and geometry of constituting polymeric chains. At temperatures above T_g, one can distinguish, in the free volume, the 'hole' component characterised by zero energy expenditure for redistribution (*i.e.*, motion) of FVE and the interstitial component that becomes accessible to transport owing to energy fluctuations greater than kT. At temperatures below T_g, yet another component of the free volume appears corresponding to the nonequilibrium thermodynamic state of glassy polymers.[4,5]

Elaboration of additive incremental (group contribution) methods for inclusion of the effect of the chemical structure of polymers on their properties became an important step towards establishment of relations between the free volume and physical properties of polymers. These methods were developed to correctly estimate the occupied volume in the polymer, which makes it possible to calculate the macroscopic free volume using the van der Waals atomic radii and particular concepts of chain packing in polymer.[6–8] Here, the calculated free volume is considered as the property of solely the polymer; however, only a fractional free volume 'sensed' by different molecular probes can be estimated.[9] This group of methods is useful for constructing correlations between the free volume and various characteristics of polymers (*e.g.*, gas diffusion and permeability coefficients), but their analysis is beyond the scope of the present review because our goal is to consider methods for investigation (first of all, experimental) of the free volume on the microscopic (molecular) level.

In connection with the development of methods of computer simulation of polymers, the fractional free volume and related notions had to be redefined more rigorously.[10,11] These methods treat polymeric chains as consisting of rigid atomic spheres with the corresponding van der Waals radii. The occupied volume (V_{oc}) is the total volume of the polymeric chains in the region under study. The unoccupied volume (voids) is defined as the volume including all points lying outside the van der Waals atomic spheres that form the polymer. Thus, the specific volume (V_{sp}) of the polymer can be represented by the sum of the occupied and void volume. Because free volume calculations are most often carried out in connection with analysis of gas diffusion, a very important notion 'accessible volume' (V_{ac}) was introduced. The accessible volume is the volume including the points that can be occupied by the centres of mass of penetrant molecules without overlap between the van der Waals volumes of the penetrant molecules and the atoms of the polymeric chains. Hence, it follows that the accessible volume is the property of the polymer – gas system, *i.e.*, V_{ac} in a given polymer will be considerably different for, *e.g.*, He and Xe atoms. It should be noted that the void volume is the

Yu P Yampolskii A V Topchiev Institute of Petrochemical Synthesis, Russian Academy of Sciences, Leninsky prosp. 29, 119991 Moscow, Russian Federation. Fax (7-495) 230 22 24, tel. (7-495) 955 42 10, e-mail: Yampol@ips.ac.ru

Received 7 February 2006
Uspekhi Khimii **76** (1) 66 – 87 (2007); translated by A M Raevskiy

property of each polymer. The accessible volume forms clusters in the interior of the polymer, the cluster size and geometry being significantly different for different penetrants.

Experimental investigations of the free volume in polymers are often carried out using probe methods. Common features of these techniques consist of introducing certain molecules (probes) into the polymer and monitoring their behaviour. The results of observations allow conclusions about the structure of the free volume to be drawn. These methods use probes of different nature and size and provide differently detailed information. For instance, in ^{129}Xe NMR spectroscopy the only probe (^{129}Xe atom) 'explores' the free volume in different polymers. In studies of polymers by positron annihilation lifetime spectroscopy (PALS), an electron-positron pair (positronium atom) serves as a probe. In inverse gas chromatography (IGC), the role of probes is played by series of structurally similar compounds.

The present review concerns the principles, fields of possible applications and results obtained by different probe methods of investigation of the free volume. The chemical formulae and names of the polymers mentioned in the text are listed in the Appendix.

II. Positron annihilation lifetime spectroscopy

Positron annihilation lifetime spectroscopy allows one to obtain information on the size, size distribution and concentration of free volume elements as well as on the effect of temperature, pressure, mechanical deformations and phase compositions of polymers on the free volume.[12–15] This method makes it possible to follow changes in the free volume occurring in the course of physical ageing of polymers, as a result of sorption and swelling and during cross-linking. Parameters of positron annihilation lifetime spectra strongly depend on the polymer structure but only slightly depend on the molecular mass,[16] which facilitates comparison of different polymers. In addition, these parameters are fairly reproducible in studies of different polymer samples and, as showed investigations carried out in different research laboratories, in the experiments with reference samples.[17]

The PALS method is based on measuring the positron lifetimes in matter. In polymers, positrons can exist in both free (e^+) and bound states, the latter being represented by H-like positronium atom, *i.e.*, an electron–positron pair (Ps or e^-e^+). The singlet state of this species, *p*-Ps, has antiparallel spins and a short lifetime (0.125 ns in vacuum), whereas the triplet state, *o*-Ps, with parallel spins has a much longer lifetime (142 ns in vacuum). It is believed that long-lived species, *o*-Ps, appear in the regions with reduced electron density (*i.e.*, in the FVE).[18–20] Due to overlap between the wave functions of *o*-Ps and electrons of atomic groups that form the FVE walls, the *o*-Ps lifetimes become much shorter compared to annihilation in vacuum, lying usually in the range from 1.5 to 4.0 ns. The observed lifetimes depend on the FVE size, namely, the larger the FVE the longer the positron lifetime in the polymer. The lifetime spectrum is a set of experimental characteristic times τ_i (ns) and corresponding statistical weights or intensities I_i (%). It is assumed that the intensity of the positronium component depends on the concentration of FVE, although it can also be affected by other factors.

Usually, ^{22}Na isotope with a half-life time of 2.6 years serves as a source of positrons. Particles formed are characterised by energies distributed between zero and 0.540 MeV with a maximum at $\sim$0.2 MeV and a mean free path of $\sim$1 mm in conventional polymers. In matter, positrons are rapidly (within $\sim$10 ps) thermalised and all subsequent processes involve particles with thermal energies.

An experimental setup for measuring positron annihilation lifetimes (see Fig. 1) consists of a source of positrons placed between two samples of the polymer under study (a plate, a stack of films or a powder). The lifetimes are measured using an electronic system (time–amplitude converter). The circuit measures the time interval between two events, namely, the appearance

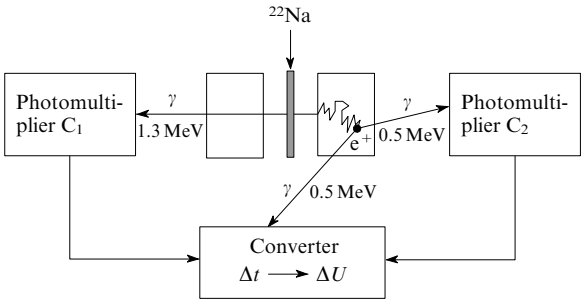


Figure 1. Scheme of a setup for measuring positron annihilation lifetime spectra.

of primary γ-quanta from the source and the appearance of quanta that accompany positron annihilation. Once detected a total of 10^5-10^7 events by a photomultiplier, an experimental positron lifetime distribution curve $y(t)$ is plotted, which shows the number of events y as function of the time elapsed t (Fig. 2).

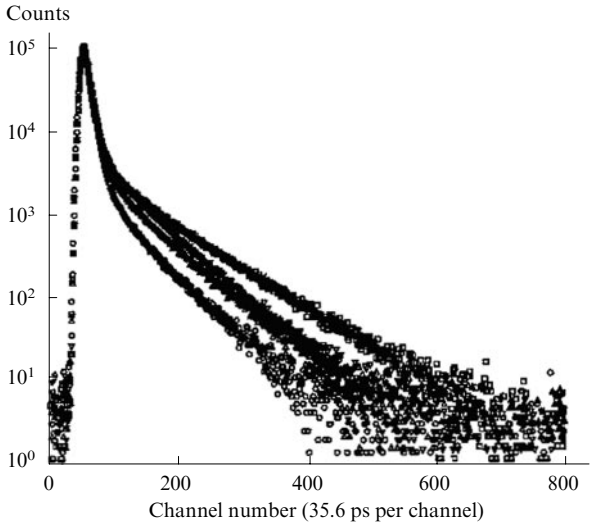


Figure 2. Typical experimental positron annihilation lifetime distributions of various polyimides.[21]

The primary experimental dependences $y(t)$ can be interpreted in the framework of analysis based on a discrete or continuous model. In the former case, the $y(t)$ curve is represented by the sum of several exponents

$$I_i \lambda_i \exp(-\lambda_i t), \tag{1}$$

where I_i is the intensity (in %) and $\lambda_i = 1/\tau_i$ (in ns^{-1}) is the annihilation rate. The number of exponents n is set in such a manner that the deviation from the experimental $y(t)$ curve be minimum. Traditionally, it is assumed that $n = 3$, although for many polymers studied recently one has $n > 3$. The first two spectral components τ_1 and τ_2 (times $\sim$0.1–0.2 and $\sim$0.3–0.5 ns, respectively) are due to annihilation of *p*-Ps and the free e^+, being not related to probing of the free volume in polymers. At the same time, the 'long-lived' components τ_i ($i = 3$ or 4) are due to annihilation of *o*-Ps located within the FVE. It is analysis of these spectral components that forms the basis for the use of PALS as probe method. Discrete analysis of primary data is performed using different programmes, *e.g.*, PATFIT.[22] Continuous data analysis using the CONTIN[23,24] or MELT[25] programmes gives the probability density function of positron annihilation characterised by a given lifetime in the polymer.

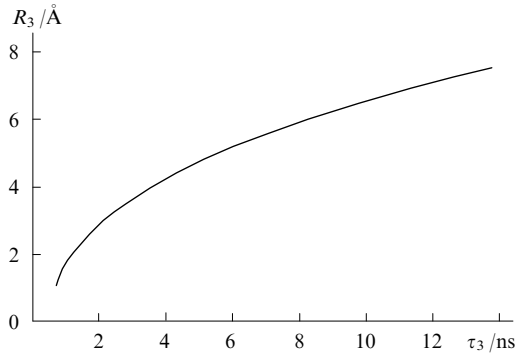


Figure 3. Correlation between positronium lifetime and average FVE radius in polymers according to the Tao – Eldrup relationship.

Here, the number of components in the lifetime spectrum is chosen by the programme automatically.

A semiempirical expression relating the lifetime of *o*-Ps (τ_3) to the average radius (R_3) of a spherical FVE in a polymer (the Tao – Eldrup relationship)[19,20] has the form

$$\tau_3 = \frac{1}{2}\left[1 - \left(\frac{R_3}{R_0}\right) + \frac{1}{2\pi}\sin\left(\frac{2\pi R_3}{R_0}\right)\right]^{-1}, \qquad (2)$$

where $R_0 = R_3 + \Delta R$ (the fitting parameter $\Delta R = 1.66$ Å was determined from analysis of the data for media with the known 'hole' size including zeolites). The FVE radii increase almost linearly as τ_3 increases (see Fig. 3).

A similar relationship is used in the case of several lifetimes of *o*-Ps. Assuming spherical geometry and a known radius, the FVE volume (v_f) or the volume distribution are found

$$v_f = \frac{4\pi}{3} R_3^3 .$$

The assumption of spherical geometry of FVE in polymers seems to be somewhat incorrect (see Section VI). Cylindrical and ellipsoidal FVE were also considered and the corresponding relations for calculating the FVE volumes from the known *o*-Ps lifetimes are available in the literature.[26–29] However, most probing studies of free volume in polymers were carried out using the Tao – Eldrup relationship.

Variations of the free volume in polymers can be illustrated by the data listed in Table 1. Here, the polymers are arranged in almost the same order as the gas permeability and radius R_3 increase. The barrier materials (*e.g.*, Vectra copolyester) are characterised by the smallest size of FVE. As the gas permeability increases, the lifetimes of *o*-Ps and the FVE size increase. It was established (see, *e.g.*, Ref. 33) that the conventional glassy polymers have a monomodal size distribution of FVE (*i.e.*, the *o*-Ps lifetime spectrum includes one time τ_3) and the lifetime distribution can be represented by Gaussian peaks when analysing the data using the CONTIN programme. However, statistical processing of spectra reveals bimodal lifetime and FVE size distributions that appear starting with particular free volume and gas permeability values (Fig. 4). For instance, the long-lived components in the lifetime spectra of PVTMS and certain relatively high-permeability polyimides[36] have a 'shoulder' or superposition of two Gaussian peaks, whereas two *o*-Ps lifetimes appear, namely, τ_3 and τ_4 (see Fig. 4) for polymers with even greater permeabilities. When treated with the CONTIN programme, maxima in the curves coincide with the lifetimes obtained by discrete processing of the primary data. Bimodal (or even polymodal) FVE size distributions were found in numerous studies of highly permeable polymers.[37–42] Note that the average FVE size and the size distribution determined from PALS data are consistent with the data obtained by other probe methods and with the results of

Table 1. Gas permeability coefficients (P_{O_2}) and FVE size in glassy polymers.

Polymer	P_{O_2} /Barrer [a]	R_3 /Å	v_{f3} /Å^3	R_4 /Å	v_{f4} /Å^3	Ref.
Vectra copolyester	0.0005	2.1	39	–	–	30
PMMA	0.09	2.6	74	–	–	31
PS	2.9	2.9	102	–	–	32
PC	1.6	2.94	106	–	–	33
Polyimides						
6FDA-ODA	2.4	3.19	136	–	–	34
6FDA-BAAF	14.2	3.62	198	–	–	34
PVTMS	44	3.21	138	4.35	345	35
PTMSS	56	2.71	83	3.74	219	35
PPrSiDPA	230	3.83	235	6.38	1088	35
AF2400	1140	2.68	81	5.95	882	35
PTMSP	7700	3.41	166	6.81	1323	35

[a] 1 Barrer = 10^{-10} cm^3 (normal conditions) cm cm^{-2} s^{-1} (cm Hg)$^{-1}$; this is the flow of gas taken by a volume of 1 cm^3 under normal conditions through a surface area of 1 cm^2 of a membrane 1 cm thick per s at a pressure drop of 1 cm Hg.

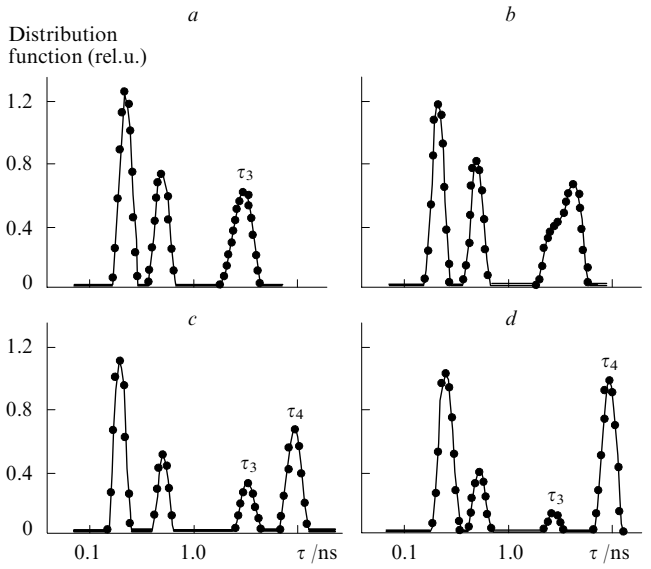


Figure 4. CONTIN positron lifetime distributions obtained for glassy polymers with the increasing free volume.[35]
Polymer: PFPDMSS (*a*), PVTMS (*b*), PPrSiDPA (*c*), and PTMSP (*d*).

molecular dynamics (MD) simulation of the free volume in polymers (see Sections IV and VI).

Free volume elements of even larger sizes were found in polymeric sorbents and organic clusters. In particular, PALS data showed that hypercross-linked polystyrene sorbents contain cavities with a radius of 14 Å and their content is ~20% of the total number of FVE in the material.[43,44] A cluster prepared by the reaction of terephthalic acid with chromium nitrate, hydrogen fluoride and water has pores ~3 nm in diameter and a specific surface area of 5900 m^2 g^{-1} (Ref. 45). This is much larger than the maximum specific surface area in zeolites. Even larger cubic cavities (volume is ~8000 Å^3) were identified in the crystal lattice of a phthalocyanine macrocycle.[46] Similar cavities probably form an open system of pores, which is important, in particular, for separation processes in membranes.

Thus, the PALS technique provides a microscopic description of the free volume in terms of the average FVE radii and corresponding volumes v_f. To relate these parameters to macro-

scopic characteristics of polymers, one should know the average FVE concentrations N (cm^{-3}) and then estimate the fractional free volume (FFV) as the product $v_f N$. This can be done using various approaches.

According to the simplest early models,[32,47,48] the intensity I_3 was assumed to be proportional to N. Then, if we know the coefficient of proportionality, A, from independent data, the concentration N is given by

$$N = AI_3,$$

and therefore one gets

$$\mathrm{FFV} = AI_3 v_f.$$

However, a more correct treatment showed that the intensity I_3 also depends on the probability of o-Ps formation, trapping rate of o-Ps by FVE and on the 'decay' of positronium under the action of polar groups (*e.g.*, C=O groups in imidazole rings of polyimides).[35] Because of this, the simple model mentioned above is no longer used. A number of more reliable methods of determination of the parameter N were developed.

1. The temperature dependences of τ_3 and FVE volume are very similar to the classical dilatometric curves for polymers, *i.e.*, the temperature dependences of the specific volume that determine the volumetric expansion coefficients of polymers. However, there is a significant quantitative difference between these dependences. Namely, the thermal expansion coefficients of a polymer (*i.e.*, its specific volume) below and above T_g (α_g, α_r) are of the order of 10^{-4} K^{-1}, whereas the thermal expansion coefficients of the free volume (α_{hg}, α_{hr}) are an order of magnitude larger. A natural explanation for this fact is as follows: the α_g and α_r values characterise the thermal expansion of both the FVE and the more dense matrix (walls surrounding the FVE). By comparing the temperature dependences of the specific volume V_{sp} and τ_3 (or v_f) one can choose N values suitable for both dependences, *i.e.*, one can determine the parameter N.[49–52] Recently, this approach was systematically used for estimating the concentration N in various amorphous polymers.[49,53,54] It was shown that in most cases the concentrations N depend only slightly on the chemical structure of polymers and their values lie in the range $(2–8)\times10^{20}$ cm^{-3} at $T = T_g$ and show a relatively weak temperature dependence.

2. The N values can also be determined from PALS data obtained in studies of gas sorption by polymers. The time τ_3 is shortened upon gas sorption. This can be interpreted as a result of selective sorption by FVE of different sizes. Because the amount of gas molecules sorbed by polymers in the course of sorption experiments under different conditions is known, Kirhheim and co-workers [55] postulated different types of FVE size distributions and estimated the N values that are consistent with the dependences $\tau_3(p)$ and $I_3(p)$, where p is the pressure. However, the N values for polycarbonate and tetramethylpolycarbonate lie in the range $(2–4)\times10^{21}$ cm^{-3} and seem to be overestimated. Indeed, they correspond to the situation where the fractional free volume in these polymers is from 30% to 100%. Here, the polymer volume per FVE should be 200 $Å^3$, which corresponds to a cube with a nearly 6 Å-edge. With allowance for the average FVE diameter this means that the neighbouring FVE should nearly contact one another, thus indicating an open porosity, which does not occur in these polymers. An attempt to estimate the parameter N from the results of sorption experiments gave a more realistic value of 4×10^{20} cm^{-3} for three polycarbonates.[56]

3. Yet another method of estimation of the N value is based on detailed analysis of the kinetics of formation and annihilation of o-Ps in polymers.[57,58] According to this approach, only a fraction of positrons that form o-Ps contributes to the long-lived component of the PAL spectrum. Therefore, the intensities I_3 and I_4 should depend not only on N, but also on the probability of trapping of o-Ps by FVE. The trapping rate is given by equation

$$v_i^t = 4\pi D_{Ps} R_i N_i \quad (i = 3, 4), \tag{3}$$

where D_{Ps} is the diffusion coefficient of non-localised o-Ps and N_i is the concentration of a particular type of traps (FVE) of radius R_i.

To determine N_i, one should know the coefficient D_{Ps} from independent data. The D_{Ps} estimates available in the literature [31] lie in the range $(0.5–15)\times10^{-5}$ cm^2 s^{-1}. Probably, the value $D_{Ps} = 1.3\times10^{-5}$ cm^2 s^{-1} obtained for polyimides [49] is the most reliable, because it is consistent with the N values determined from the temperature dependence of τ_i below and above T_g. Of course, one should also know how the coefficient D_{Ps} varies for different polymers. Analysis of the D-*vs.*-d^2 dependences (D is the diffusion coefficient of molecules with the gas-kinetic diameter d lying between 2.5 and 4 Å) for different polymers showed that extrapolation to the o-Ps size ($\sim$1 Å) gives the diffusion coefficients that fall in a relatively narrow range of one decimal order of magnitude.

The concentration N in partially crystalline polymers can be estimated from the densities of polymers of different crystallinity.[59] Assuming that the specific volume of the crystalline phase equals the occupied volume, one can determine the fraction of the specific volume of the amorphous phase h. Then N is given by

$$N = \frac{h}{v_h}, \tag{4}$$

where v_h is the average FVE volume found from PALS data.

At last, the N values for polymeric sorbents and some high-permeability open-pore polymers can be estimated from joint analysis of the annihilation parameters and pore size distribution obtained according to Brunauer–Emmet–Teller.[43]

An indirect estimate of N can be obtained using the average size of FVE in polymers. The average volume of the polymer matrix per FVE in a polymer should be much larger than the FVE volume. Assuming that the specific volume of the polymer is about 1 cm^3 g^{-1} and N is nearly $\sim10^{20}$ g^{-1} (or $\sim10^{20}$ cm^{-3}), one gets the volume per FVE $v = 10^4–10^3$ $Å^3$. This corresponds to a cube with a 20–10 Å-edge. The average diameter of FVE in polymers is $\sim$5–13 Å; therefore, one can conclude that the average distance (k) between neighbouring FVE is 5 to 10 Å. At much smaller k values, the regularities of gas transport in polymers will be similar to those in porous media, which contradicts the majority of experimental data. At $N > 10^{21}$ cm^{-3}, the parameter k should take negative values. Note also that the k values determined are in good agreement with the diffusion jump lengths of gas molecules in polymers estimated using the Meares model.[60] The values of N obtained by different methods for different polymers are listed in Table 2.

Table 2. FVE concentrations in different polymers according to PALS data.

Polymer	$10^{-20}N$ /cm^{-3}	Ref.
PE	6–8	59
Polyolefins	5	61
EVA	6, 7	62
Rubbers	2–6	52
PVC (plasticised)	8	54
PC	40	55
	6–11	50
	4	56
PVTMS, PTMSP, AF2400, AF1600, PTMSS, *etc.*	6–15	35, 49
Poly(ether imides)	4–8	49

Thus, the PALS technique allowed one to obtain a fundamental result, namely, the FVE concentration in all polymers lies in a narrow range from 10^{20} to 10^{21} cm^{-3}.

1. Free volume in thin films and on the surface of solids

Traditionally, the PALS method is used in studies of the free volume inside a polymer matrix. However, there is a variety of objects [free thin polymer films (membranes), coatings on the surface of various materials, *etc*.] for which the surface rather than bulk properties of polymers are important. Glass transition temperature,[63,64] density,[65,66] chain mobility and some other characteristics[67] of polymers measured for the bulk phase (polymer matrix) and at interfaces can be significantly different.

Positrons used in traditional version of the PALS technique have an average energy of 200 keV and a braking distance of $\sim$1 mm. The latter value is several orders of magnitude larger than the characteristic thickness of surface layers; therefore, the positron lifetimes in PALS experiments contain information on the free volume in the matrix. Studies of the free volume in near-surface layers require that the positron beam energy be much lower than 200 keV (positrons should not penetrate into the interior of the sample and annihilate in the near-surface layers). The development of monochromatic low-energy positron beam techniques[68] with much lower controllable positron energies (0.2–20 keV) made it possible to probe the free volume in thin polymer layers (of the order of a few nanometres) and to plot the corresponding free volume profiles.

The surface layers at polymer–vacuum interfaces have been best studied,[69,70] whereas investigations at the polymer–polymer interface are less detailed.[71] As the positron energy decreases, the *o*-Ps lifetimes (τ_3) in different glassy polymers [an epoxide copolymer, polystyrene, poly(methyl methacrylate)] increase compared to the lifetimes measured in conventional PALS experiments where the depth of position penetration is larger.[69,70,72,73] Taking into account the Tao–Eldrup relationship, this suggests an increase in the size of FVE in the near-surface layers. Using the density profile, it was shown[71] that there is a variable-density layer 30–40 Å thick near the interface where the size of FVE does increase. The FVE size distribution is broadened near the polymer–vacuum interface.[70] An unexpected result was obtained for polystyrene, namely, a bimodal positron lifetime distribution with τ_4 values lying in the interval from 8 to 14 ns was revealed,[71,72] which corresponds to FVE size from 5.7 to 6.2 Å and exceeds considerably the size of FVE in polystyrene matrix. However, it cannot be ruled out that we deal with an artifact due to superposition with positron annihilation in vacuum characterised by much longer Ps lifetimes.

Yet another observation has no reasonable explanation so far. In addition to a very thin near-surface layer (a few tens of ångström thick) characterised by densification with an increase in the distance from the interface, there is a much thicker (a few micrometres) layer the density of which decreases as the distance from the interface increases. This is indicated by changes in the densities of glassy polymers and in the coefficients of gas diffusion therein.[65,66] Probably, harmonisation of these data requires further studies.

2. Effect of chemical structure on the free volume in polymers

Analysis of the results of numerous PALS studies showed that the free volume in polymers is highly sensitive to the chemical structure of the monomer unit. That is why the gas permeability and gas diffusion coefficients of polymeric materials depend on their structure (Table 3).

An efficient method of increasing the free volume of a polymer consists of introducing bulky substituents [first of all, $Si(CH_3)_3$ groups] into the main chain (see the data for two metathesis-derived polynorbornenes in Table 3). The introduction of other substituents (*e.g*., a methyl group) into aromatic nuclei of the main chain also causes a systematic increase in the positron lifetime and FVE size (in Table 3, this can be followed using the data for polyimides and polycarbonates).

Table 3. Effect of polymer structure on lifetimes τ_3 and FVE radii.

Polymer	τ_3 /ns	R_3 /Å	Ref.
Poly(norbornene)	2.15	2.9	74
$(CH_3)_3Si$-Substituted poly(norbornene)	2.70	3.4	75
6FDA-Polyimides with different number of methyl groups (*n*) in phenylenediamine residue			76
$n = 0$ (6FDA-PDA)	2.57	3.3	76
$n = 1$ (6FDA-1)	2.80	3.5	76
$n = 2$ (6FDA-2)	3.15	3.7	76
$n = 3$ (6FDA-P14)	3.63	4.0	76
$n = 4$ (6FDA-P13)	3.94	4.2	76
Polycarbonate	2.1	2.9	33
Tetramethylpolycarbonate	2.4	3.2	33

3. Effect of temperature

The temperature dependences of Ps lifetimes were mentioned above in connection with the estimation of FVE concentration in polymers. Numerous studies (see, *e.g*., Refs 33, 47, 52–54, 77, 78) showed a linear increase in τ_3 in the glassy-state region followed by a kink near T_g and subsequent linear increase in τ_3 (with a greater slope) in a highly elastic state with an increase in temperature. This is illustrated in Fig. 5. Most polymers are characterised by thermal expansion coefficients of FVE of 1×10^{-3} K^{-1} below the glass transition temperature and $(2-10) \times 10^{-3}$ K^{-1} above T_g (see Refs 52, 53 and 77).

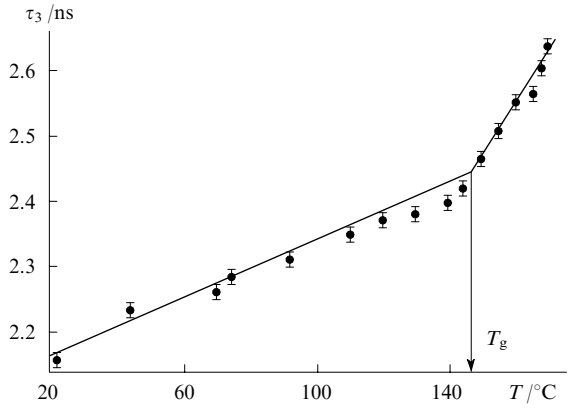


Figure 5. Temperature dependence of positronium lifetime τ_3 in polycarbonate.[78]

Interestingly, some polymers present exceptions. For instance, a study of PTMSP (polymer with the largest FVE and record high gas permeability) showed that the times τ_3 and τ_4 are independent of temperature.[39] Probably, for this polymer the effect of temperature on small-scale motions of atomic groups in the FVE walls (these motions should govern the temperature dependences of τ_3 in conventional glassy polymers) is less pronounced due to abnormally large FVE size. Substantiation of this hypothesis requires additional measurements of the $\tau_i(T)$ dependences for other polymers with large free volumes.

4. Effect of pressure

The nanostructure of the free volume (average FVE radius and FVE size distribution) in polymeric materials can be significantly changed by applying high pressure. These changes are well 'sensed' by the PALS technique. In particular, the average FVE

radius in polyepoxide decreases from 2.5 to 0.73 Å and the FVE size distribution becomes narrower as the pressure increases from 0 to 14 kbar.[79] The effect of high pressure on the polymer also manifests itself as an aftereffect, namely, the lifetimes τ_3 and corresponding FVE size decrease after decompression.[48,80,81]

5. Mechanical effects

The PALS method is also suitable for probing changes in the free volume (cavity size and concentration) due to deformation of polymers. However, because orientation of polymeric films can be accompanied by crystallisation and the changes in the supramolecular structure and in FVE geometry, interpretation of experimental data can be ambiguous. If deformation of amorphous polymers (*e.g.*, polycarbonate[78]) at room temperature causes no crystallisation at small relative elongations (less than 2%, *i.e.*, in the region of quasielastic deformation), the time τ_3 linearly increases with the relative elongation thus indicating an increase in FVE. At the same time biaxial orientation of poly(ethylene terephthalate), poly(ethylene naphthenate) and their copolymers at temperatures above T_g causes only minor changes in τ_3 and I_3 and significant changes in the gas permeability and diffusion coefficients. This points to predominance of sample morphology (lengthening of 'diffusion paths').[82] Much greater changes in the annihilation parameters were observed at larger relative elongations Δl upon deformation of partially crystalline polymers (taking polyethylene as an example).[83] As Δl increases, the positron lifetime, τ, corresponding to the fractional free volume in the amorphous phase initially decreases and then (at large Δl) remains unchanged. It was assumed that the changes in τ characterise a change in the shape of FVE from nearly spherical in undeformed sample to ellipsoidal in oriented polymer. Other examples of PAL studies of mechanical effects in polymers can be found in the review.[15]

One of the first PAL studies of the phenomena accompanying deformation of polymers was reported by Askadskii *et al.*[84] Unfortunately, the authors studied a polyimide based on pyromellitic dianhydride and 4,4′-diaminodiphenyl oxide, which is also known as Kapton polyimide. This and numerous subsequent studies (see, *e.g.*, Refs 31, 85 and 86) revealed that the PAL spectrum of this polymer shows only one relatively short-lived component (lifetime 0.3 – 0.4 ns) instead of three components. It is noteworthy that this feature allows Kapton polyimide to be used as a component of the source of positrons, because Kapton films do not change the positron lifetimes in the sample under study. Apparently, this is due to the fact that at high concentration of dicarboximide rings in this polymer the positronium production is efficiently inhibited through trapping of positrons by the ring carbonyl groups. As a result, annihilation mainly involves free positrons and occurs in relatively close-packed polymer domains rather than FVE. Again, the absence of the long-lived component ($I_3 = 0$) shows that the parameter I_3 cannot serve as a measure of FVE concentration, because it depends on the positronium yield. Otherwise, Kapton should be characterised by zero free volume, whereas the gas diffusion coefficients for the polymer are similar to those found for other polymers (*e.g.*, $D_{O_2} = 0.29 \times 10^{-8}$ cm^2 s^{-1} according to Ref. 87). Also note that the absence of the τ_3 component can be due to a decrease in the FVE concentration owing to an increase in the concentration of cross-links, as shown for oligo(ester acrylates).[88]

III. ^{129}Xe NMR spectroscopy

Chemical shifts in the ^{129}Xe NMR spectra are highly sensitive to the free volume in the medium where gaseous xenon is sorbed. Qualitatively, the larger the FVE size the smaller the ^{129}Xe chemical shift relative to the chemical shift characteristic of the gas phase. In this respect, polymers differ insignificantly from other condensed media, namely, large chemical shifts are observed in, *e.g.*, the media with high refractive indices. In this connection we can say that the xenon atom placed inside the FVE is in a local low-refraction medium and characterised by a smaller chemical shift.[89]

Note that the ^{129}Xe chemical shift is sensitive to structural and morphological features of partially crystalline and cross-linked polymers, polymer blends and block copolymers; it also changes near the glass transition temperature.[90–97]

According to Fraissard and co-workers[98,99] who studied the sorption of xenon in various zeolites, the chemical shift in the NMR spectrum of a ^{129}Xe atom sorbed in nanoporous medium in the absence of paramagnetic species or admixtures producing a strong local electric field (*e.g.*, cations) can be writen as folows:

$$\delta_\Sigma = \delta_0 + \delta + \delta_{Xe/Xe}\rho, \tag{5}$$

where δ_0 is a constant, δ is the chemical shift due to collisions with the FVE walls, $\delta_{Xe/Xe}$ is the chemical shift due to collisions with other xenon atoms in the gas phase and ρ is the density of the gas phase. Therefore, after extrapolation to zero pressure of gaseous xenon the difference

$$\delta = \delta_\Sigma - \delta_0$$

should characterise only the collisions with the walls within the FVE. Based on analysis of the data for zeolites, an empirical relation for the experimentally measured chemical shift was proposed[98]

$$\delta = \frac{499.1}{2.054 + \lambda}, \tag{6}$$

where λ (in Å) is the mean free path of a xenon atom within the FVE. Note in advance that this method is only applicable to studies of those FVE the size of which exceeds that of the xenon atom. Assuming different FVE geometries, from the λ value one can estimate the diameter of either a spherical cavity (D_{sp}) or a cylindrical FVE (D_c) with a large length-to-diameter ratio,

$$\lambda = \frac{D_{sp}}{2} - 2.2, \tag{7}$$

$$\lambda = D_c - 4.4. \tag{8}$$

The free terms in relations (7) and (8) are the radius and diameter of the xenon atom, respectively. This approach is based on the possibility of determining the size of the lattice cell from X-ray diffraction data for zeolites[100] and availability of various characteristics of xenon. By extending relationships (6) – (8) to other nanoporous systems (in particular, polymers) it is possible to estimate their FVE sizes. However, it should be noted that there are some difficulties related to, *e.g.*, a large scatter of numerical characteristics of the size of xenon atom determined by different methods (see details below).

The FVE size was determined from the results of ^{129}Xe chemical shift measurements of xenon sorbed in different polymers. NMR measurements were carried out at low pressures or extrapolation to low pressures was used. ^{129}Xe NMR data obtained assuming spherical and cylindrical FVE geometries are listed in Table 4. For comparison, we also present the results obtained by other probe methods for different polymers. Analysis of these data allows one to draw some general conclusions.

First of all, the ^{129}Xe chemical shift can be considered as a characteristic property of the polymer, as indicated by coincidence of the chemical shifts for the polymers studied by different authors (*e.g.*, for PE and PS).

Polymers studied to date can be divided into two groups. Polymers with relatively small free volume and low gas permeability are characterised by the chemical shifts (δ) in the region δ 200 – 214. This corresponds to the FVE radii lying between 2.5 and 2.9 Å, being in good agreement with the PALS data (see Table 4). Significantly smaller δ values are observed for high-permeability perfluorinated polymers.[101] Because small δ values correspond to larger FVE radii, this was interpreted as substantiation of the higher permeability of such polymers. However,

Table 4. Radii of spherical (R_{sp}) and cylindrical (R_c) FVE (Å) determined by different methods.

Polymer	^{129}Xe NMR spectroscopy					PALS			IGC	
	δ	λ /Å	R_{sp}	R_c	Ref.	R_{sp}	R_c	Ref.	R_{sp}	Ref.
AF2400	63.3	5.83	8.04	5.12	101	5.95	6.33	36	6.4	102
AF1600	76.7	4.46	6.66	4.43	101	4.89	5.43	36	5.8	103
AD 80X	83.6	3.92	6.12	4.16	101	–	–			
AD 60X	85.3	3.80	6.00	4.10	101	–	–			
PTFE	90	3.49	5.69	3.94	26	4.2	4.9	26		
PTMSP	148	1.32	3.52	2.9	89	6.8	6.5	36	–	
	178	0.75	3.0	2.6	104					
PPO	180	0.72	2.92	2.56	26	3.4	4.2	26	3.4	105
	185	0.64	2.84	2.52	106					
	188	0.60	2.80	2.50	107					
LDPE	203	0.40	2.60	2.40	26	3.3	4.1	26		
	200	0.44	2.64	2.42	90					
	200	0.44	2.64	2.42	97					
PC	214	0.28	2.48	2.34	26	2.9	3.8	26		
	212	0.30	2.50	2.35	90					
PS	210	0.32	2.52	2.36	108	2.88	3.76	33		
PEMA	203	0.40	2.60	2.40	97	3.0	3.9	109		

other factors affecting the chemical shift can exist. This is indicated by the δ values measured for PTMSP (polymer with the largest free volume and record high gas permeability).[89, 104] Typical of perfluorinated polymers are relatively low refractive indices n_D equal to $\sim$1.3, which corresponds to the molecular refraction

$$R_m = \frac{n_D^2 - 1}{n_D^2 + 2} = 0.187,$$

whereas conventional polymers (*e.g.*, PS, PC, PEMA) are characterised by n_D value lying between 1.5 and 1.7 (molecular refraction is $\sim$0.3–0.4).[110] One can assume that the ^{129}Xe nuclei arrive at regions with lower refraction upon collisions with the FVE walls in perfluorinated polymers, *i.e.*, the lower polarisabilities of chemical bonds in these materials cause less pronounced perturbations of ^{129}Xe nuclei.[89] The aforesaid suggests that the FVE radii calculated from relations (6)–(8) and listed in Table 4 seem to be somewhat overestimated. This does not contradict the PALS and IGC data that are also shown in Table 4. Only PTMSP presents an exception, namely, the FVE size estimates for this polymer not only do contradict the data for other polymers, but are also inconsistent with the PALS data. Probably, errors in estimation of the FVE size from expressions (7) and (8) are due to the complex geometry of the free volume in PTMSP.[111]

The second problem is related to uncertainty in the size of the xenon atom, which is used for estimation of FVE. Different methods of determination of the atomic diameter (d) of xenon (from viscosity of gas, second virial coefficient, intermolecular interaction potentials, liquid and crystal densities) give the values in the range from 3.2 to 4.6 Å (values obtained before 1990 were summarised in Ref. 112). Traditionally, it is accepted that d equals 4.4 Å (this value was obtained using the van der Waals radii corrected by Pauling and reported by Breck [100]). However, Breck also reported a smaller value (3.96 Å) calculated using the Lennard-Jones potential of intermolecular interactions. The data listed in Table 5 illustrate the effect of d value on the theoretical radius of spherical FVE for two polymers with large free volume. Clearly, agreement with the data obtained by other probe methods is more or less depending on the d value chosen. However, a broad FVE size distribution found from MD simulation suggests that the FVE radii mentioned above fall in the range of possible values.

The results of experiments on encapsulation of ^{129}Xe atoms in C_{60} fullerene and measurement of ^{129}Xe NMR spectrum [113] offered some prospects for refinement of the ^{129}Xe NMR data (see above). On the one hand, the synthesis of inclusion compound

Table 5. Atomic diameter of xenon and FVE radii obtained by different methods.

δ	λ /Å	d /Å	R_{sp} /Å			Ref.
			^{129}Xe NMR spectroscopy	PALS	MDS /Å (see [a])	
Polymer PTMSP						
148	1.32	3.2	2.9	6.8	2–10	89
		3.96	3.3			
		4.4	3.5			
178	0.75	3.2	2.4	–	–	104
		3.96	2.7			
		4.4	3.0			
Polymer AF2400						
63.3 (powder)	5.83	3.2	7.4	6.0	1.5–12	101
		3.96	7.8			
		4.4	8.0			
64.7 (film)	5.63	3.2	7.2	–	–	101
		3.96	7.6			
		4.4	7.8			

[a] MD simulation data were taken from Ref. 111.

Xe@C_{60} is quite unexpected, because the diameter of xenon atom (4.4 Å) exceeds that of the fullerene cavity. This could be evidence of smaller d(Xe) value. On the other hand, the measured ^{129}Xe chemical shift in this compound is δ 179.24, which gives an estimate of 5 to 6 Å for the inner diameter of the C_{60} cavity. Probably, in this case estimation from expressions (6)–(8) is not substantiated, because we can assume that the xenon atom encapsulated in C_{60} cavity will simultaneously interact with a few (probably, all) fullerene carbon atoms and this will cause large chemical shifts, thus making the Fraissard model inapplicable.[114] However, this result indicates the necessity of taking into account the interactions between xenon atom and FVE walls in polymers.

IV. Inverse gas chromatography

Inverse gas chromatography (IGC) is used to study the thermodynamics of sorption of gases and vapours in polymers and to determine their physicochemical parameters.[115, 116] To this end, a polymer is applied on the surface of a solid porous substrate and the sorbate is introduced in the carrier gas flow. Under particular

conditions, by measuring the retention times t_r one can calculate various thermodynamic parameters of the polymer–gas system.

From the known t_r values, it is possible to calculate the net retention volume V_n of a sorbate

$$V_n = (t_r - t_a)J_n^m F_c \frac{273}{T}, \quad (9)$$

where t_a is the retention time of the 'non-sorbable' component (*e.g.*, air), which takes into account the dead volume of the chromatograph; J_n^m is the correction for pressure drop in the column; F_c is the rate of the carrier gas; and T is the temperature (in K) at which the experiment is carried out.

A correct application of IGC technique in studies of bulk sorption in polymers implies no diffusion control of the chromatographic experiments; namely, the characteristic times of diffusion into the bulk of the supported polymer should be shorter than the 'effective' times of contacts of a sorbate with the polymer phase. Experimentally, this can be achieved using lower rates of the carrier gas, by applying thinner polymer films or by carrying out measurements at higher temperatures.

The main thermodynamic characteristic of bulk sorption (in contrast to adsorption on polymer surface) is the specific retention volume V_g defined as follows:

$$V_g = \frac{V_n}{\omega_L}, \quad (10)$$

where ω_L is the mass of the polymer in the column. With this parameter known, one can calculate [117] the solubility factors (S) at infinite dilution

$$S = V_g \frac{\rho}{p_0} \exp\left[(2B_{11} - V_1)J_n^m \frac{p_0}{RT}\right], \quad (11)$$

where ρ is the density of the polymer at temperature T; p_0 is the standard pressure (1 atm); the exponential term, which includes the second virial coefficient B_{11} and the molar volume of the sorbate V_1, takes into account the non-ideal state of vapours; R is the universal gas constant.

Yet another important thermodynamic characteristic determined using V_g is the activity coefficient $(a_1/w_1)_\infty$ at infinite dilution

$$\ln\left(\frac{a_1}{w_1}\right)_\infty = \ln\left(\frac{273R}{V_g p_1^0 M_1}\right) - \frac{p_1^0}{RT}(B_{11} - V_1), \quad (12)$$

where M_1 is the molecular mass of the sorbate and p_1^0 is the vapour pressure of the sorbate at temperature T.

The partial molar enthalpy of mixing, ΔH_m, characterises the sorbate–polymer interaction and can be calculated from the temperature dependence of the activity coefficient.

$$\Delta H_m = R \frac{\partial \ln(a_1/w_1)_\infty}{\partial(1/T)}. \quad (13)$$

It can also be estimated from the temperature dependence of the solubility coefficient

$$S = S_0 \exp\left(-\frac{\Delta H_s}{RT}\right), \quad (14)$$

because the enthalpy of sorption can be represented by the sum

$$\Delta H_s = \Delta H_c + \Delta H_m, \quad (15)$$

where ΔH_c is the enthalpy of condensation, which is tabulated for different sorbates.[118]

Studies of several glassy polymers [polysulfone,[119] poly(vinyltrimethylsilane),[120] poly(phenylene oxide)[105] and amorphous Teflons AF[102, 121]] showed that the ΔH_m values strongly depend on the size of the sorbate molecule. The ΔH_m values of *n*-alkanes C_3-C_{12} initially decrease as the molecular masses of these hydrocarbons increase, pass through minima at particular sizes of the sorbate molecules (these sizes are different for different polymers) and then increase again. It was assumed [122] that the critical size of the sorbate molecule, which corresponds to the minimum and the highest exothermicity of mixing, is also related to the average size of FVE. This hypothesis is substantiated by establishment of correlations between the minimum ΔH_m values and the diffusion coefficients and gas permeabilities of glassy polymers. Probably, this behaviour is due to the ability of FVE to uptake molecules with sizes smaller than the FVE size. Sorption within FVE requires no energy expenditure to overcome the intermolecular interaction forces; therefore, the observed ΔH_m values are negative. The smaller the size difference between the sorbate molecule and FVE size the softer the restrictions imposed on the internal degrees of freedom of the sorbed molecule; as a result, the entropy of mixing ΔS_m, which correlates with ΔH_m, also passes through a minimum.[122] Thus, the IGC technique permits estimation of the FVE size. The IGC data can be compared with the results obtained using other methods of investigation of the free volume.

The effect of the critical volume V_c used as a measure of the molecular size of sorbates (n-alkanes) on the ΔH_m of particular polymers is illustrated in Fig. 6 *a*. The ΔH_m values pass through minima the coordinates of which ($V_{c,min}$) are in qualitative correlation with the gas permeability and diffusion coefficient of a given polymer, namely, polymers with larger $V_{c,min}$ values are characterised by higher diffusion coefficients and gas permeabilities and *vice versa*.

Figure 6 *b* presents the FVE size distributions plotted from PALS data. The ordinate axis denotes the probability density

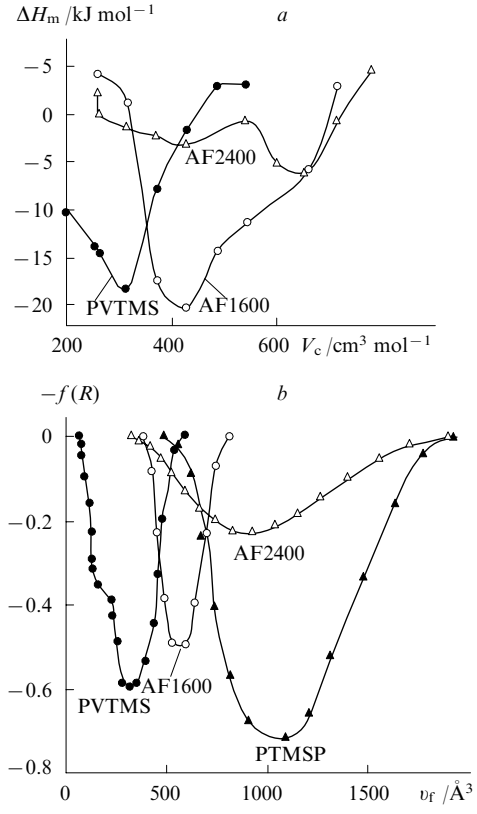


Figure 6. FVE size distribution in glassy polymers.[121]
Partial molar enthalpies of mixing plotted *vs*. critical volumes of sorbates (n-alkanes) according to IGC data (*a*) and the probability density functions $f(R)$ for polymers with FVE of different size according to PALS data (*b*).

function $f(R)$ determined using the CONTIN program. The radii of FVE were calculated for spherical geometry using the Tao – Eldrup relationship and then the v_f were found. For clear visual comparison with the dependence on V_c (Fig. 6 *a*), it is appropriate to recalculate the necessary parameters per mole of a particular compound, *i.e.*

$$v_f' = v_f N_A \ (\mathrm{cm^3\ mol^{-1}}),$$

where N_A is the Avogadro constant. A comparison of the plots shown in Fig. 6 *a* and Fig. 6 *b* shows a clear analogy between the FVE size distributions obtained by two independent methods. Consider this result in more detail.

1. The relative positions of the curves in Fig. 6 *a* and Fig. 6 *b* are very similar. Both methods assign the smallest FVE size to PVTMS and the largest one to AF2400. Minima in the $\Delta H_m(V_c)$ curves for AF1600 and PVTMS correspond to alkanes C_6 and C_7, respectively, whereas for AF2400 the minima correspond to bulkier sorbates C_{10} and C_{11} (minima at V_c and v_f' equal to $\sim 600\ \mathrm{cm^3\ mol^{-1}}$).

2. According to PALS data, polymer AF1600 has a much narrower FVE size distribution compared to AF2400. Probably, the narrower this size distribution the stricter the size segregation of the molecules sorbed in FVE. This conclusion is also consistent with the IGC data, namely, the minimum in the ΔH_m curve is much broader for AF2400 than for AF1600.

Quantitative determination of the FVE size from IGC data requires substantiated choice of the probe size (probes are the n-alkanes sorbed in polymers). To this end, different parameters can be used, *e.g.*, the van der Waals volume V_W,[123] the molar volume in the liquid phase V_b (at the corresponding boiling temperature T_b)[124] and the critical volume V_c.[125] Although these quantities are significantly different from one another (see Table 6), they show the same trend of changes among the polymer – sorbate systems studied. A comparison with other probe methods (PALS, ^{129}Xe NMR spectroscopy) and with the results of MD simulation[111] showed that the best agreement is achieved using V_b or even V_c as a measure of FVE. This is probably due to the fact that linear *n*-alkane molecules should adopt a folded conformation in order to be arranged within (postulated) spherical FVE; because of this, a rather large excluded volume should be added to the intrinsic (van der Waals) volume of the probe.

Some features and limitations of the IGC technique should be pointed. First of all, the FVE size determined using this method is found from the temperature dependence of ΔH_m, *i.e.*, the IGC method provides a temperature-averaged value. Though, with allowance for the thermal expansion coefficient of FVE (about $10^{-3}\ \mathrm{K^{-1}}$ for glassy polymers according to PALS data) these differences seem to be insignificant for the temperature intervals (nearly 100 degrees) corresponding to operating conditions. Another problem is related to a limited set of compounds suitable for free volume determination by IGC. The dependences of ΔH_m on the sorbate size in rubbers do not pass through minima due to another mechanism of dissolution and mixing. Additionally, the diffusion coefficients of many glassy polymers are insufficiently high so that the experiments are carried out with diffusion limitatious. The results obtained show that the IGC technique is applicable to free-volume studies of polymers characterised by oxygen permeabilities $P_{O_2} > 20$ Barrer at room temperature. However, the number of such polymers is rather large. Polymers with lower permeabilities can be investigated at elevated temperatures.

Table 6. Molecular volumes (Å^3 per molecule) and FVE radii (Å) corresponding to minima in ΔH_m-*vs.*-v_f plots.[126]

Polymer [a]	$\frac{V_W}{R}$	$\frac{V_b}{R}$	$\frac{V_c}{R}$
PVTMS (C_6)	$\frac{113}{3.0}$	$\frac{235}{3.8}$	$\frac{611}{5.3}$
AF1600 (C_7)	$\frac{130}{3.1}$	$\frac{269}{4.0}$	$\frac{708}{5.5}$
PDSNb (C_8)	$\frac{147}{3.3}$	$\frac{316}{4.2}$	$\frac{807}{15.8}$
AF2400 (C_{11})	$\frac{198}{3.6}$	$\frac{436}{4.7}$	$\frac{1096}{6.4}$

Note. The molecular volumes are given in the numerator and the FVE radii are given in the denominator.
[a] n-Alkane corresponding to minimum ΔH_m value is given in parentheses.

V. Miscellaneous methods

Many processes involving low-molecular-mass compounds dissolved in polymers are controlled by mobilities of these compounds. The rate of translational (or rotational) mobility strongly depends on the molecule (probe)-to-FVE size ratio in a given polymer. Therefore, by following the mobility of probes of different size in different polymers one can obtain information on the free volume.

1. The photochromic probe technique

The technique is based on a hypothesis,[127] according to which the implementation of monomolecular chemical reactions (in particular, photoisomerisation) in glassy matrices requires a minimum (critical) FFV in the immediate vicinity of the dissolved probe molecule. This method involves measurements of the degree of *cis – trans*-photoisomerisation of a probe in a glassy polymer and in a dilute solution in a model non-viscous solvent where the free volume imposes no restrictions on the isomerisation. Having determined the ratio of these parameters as a function of the probe size (more exactly, as a function of the volume necessary for isomerisation to occur), one can estimate the average size of FVE. Victor and Torkelson[128] studied the free volume in glassy polystyrene using various stilbene and azobenzene derivatives with the van der Waals volumes in the range of 127 – 571 Å^3 as probes. The implementation of photoisomerisation requires an additional volume for the rearrangement of the molecule that undergoes isomerisation in the excited state. This volume can be estimated from geometric considerations. It was found that more than 90% of the FFV in PS exceeds 120 – 130 Å^3, no FVE with size > 400 Å^3 are present, and the maximum in the FVE size distribution curve is at $\sim$270 Å^3. Assuming, as in other cases, spherical symmetry of FVE, one gets a FVE radius of $\sim$4 Å, which is somewhat larger than the values obtained using other probe methods (2.4 – 3.8 Å, see Table 4).

Data on changes in the free volume during physical ageing of glassy polymers obtained by this method worth mentioning. Larger FVE are the first to disappear in the ageing of poly(methyl methacrylate) and PS.[129] At the same time, an ageing study of polycarbonate characterised by a broader FVE size distribution showed that both large and small free-volume elements disappear simultaneously.[130]

2. The spin probe technique

This was one of the first methods used for estimating the free volume in polymers. It is based on the concept that the mobility (rotational frequency v_{cor}) of spin probes, namely, stable nitroxyl radicals, first of all 2,2,6,6-tetramethylpiperidine-1-oxyl (TEMPO), is sensitive to the dynamic or structural features of the polymers in which the probes are dissolved.[131] The probe rotational frequency v_{cor} can be estimated from EPR spectral parameters. Depending on the v_{cor} values, slow ($0.2 \times 10^9 < v_{cor} < 10^7\ \mathrm{s^{-1}}$) and fast ($v_{cor} > 0.5 \times 10^9\ \mathrm{s^{-1}}$) motions of probes in polymers are distinguished. At room temperature, the rotational frequencies of probes in rubbers decrease as

the glass transition temperature increases. Initially, it was accepted that the FVE size in glassy polymers is less than the probe size and therefore only slow motions should occur, as is the case of, *e.g.*, polystyrene. However, it was unexpectedly found that TEMPO radicals execute fast motions while larger spin probes execute slow motions in PVTMS.[132] Thus, estimation of the FVE size in PVTMS, which possesses rather high permeability, showed that it exceeds the size of the TEMPO molecule (more exactly, it is larger than the volume necessary for rotation of the TEMPO molecule by an angle of 1 radian). Later, similar relations were established by different probe methods for a number of polymers with relatively large FVE sizes.[133]

However, it was shown [134, 135] that the model for rotation used in the interpretation of the EPR spectra of the spin probes is simplified and the character of the motion and librations of spin probes in glassy polymers and low-molecular-mass glasses is more complex. Nevertheless, even assuming that the parameter v_{cor} does not reflect the actual dynamics of spin probe motions in FVE, it can be considered as an indicator of the probe-to-FVE size ratio in polymers, which shows the relative differences in the FVE values in different polymers.

3. The electrochromic probe technique

The electrochromic effect, *i.e.*, a change in colour under the action of an electric field, is due to the effect of the electric field on the light-absorption of organic compounds. Orientation of light-absorbing molecules in an electric field changes their extinction coefficients. This can be used for estimating the molecular mobility or the free volume in polymers.[136] To this end, the light-absorbing molecules acting as probes are dissolved in polymers. Experiments involve detection of changes in the extinction coefficients upon switching the electric field on and then off when random reorientation of the dissolved probe molecules occurs. To make the effect more pronounced, the probe molecules should have large dipole moments, *e.g.*, azo dyes with the van der Waals volumes lying in the range of 770 – 2900 Å^3.[137] Note that so large probe sizes correspond to hypothetical FVE sizes that are absent in real polymers. In addition, molecules with large dipole moments can strongly interact with polar groups in the polymer structure. Therefore, the electrochromic probe technique is not a 'non-perturbative' one, *i.e.*, the FVE size thus determined should sense distortions produced by the introduction of the probe molecules. Nevertheless, the results obtained by this method were useful in the early stages of investigations of the free volume in polymers.

To estimate the average FVE size, one has to analyse the kinetic curves of changes in the optical density upon orientation of dipoles by the electric field and after switching this field off. Experiments are carried out with probes of different sizes. The FVE size is determined using the Cohen – Turnbull model.[2, 3]

Studies of glassy polymers (PS, PVTMS and PTMSP) [138, 139] using the electrochromic probe technique gave a 'correct' order of changes in the free volume in these polymers, *i.e.*, its increase with an increase in the gas permeabilities and diffusion coefficients. Interestingly, the temperature dependence of the average FVE size in PTMSP was found to be an order of magnitude weaker than in PS; this was confirmed by PALS data.[39]

The average FVE size in PS was found to be in good agreement with that obtained by the photochromic probe technique.[128] However, studies by both methods were carried out using very large probes; therefore, it cannot be ruled out that the FVE sizes are overestimated. For instance, the value v_f = 3290 Å^3 found for PTMSP corresponds to a spherical cavity with the radius of 9 Å. This exceeds considerably the value obtained from PALS data for this polymer (according to results of MD simulation, the presence of so large cavities seems not to be improbable, see Section VI). Based on the aforesaid, data of free-volume studies carried out using large probes should be analysed with special care. Additionally, when comparing different polymers taking into account the matrix-perturbing effects, it is more correct to consider the probe mobility as a semiquantitative characteristic of the free volume.

4. The conformation probe technique

To probe the free volume in polymers, it was proposed to use organic compounds that can exist as two conformers with different IR spectra.[140 – 142] The FVE size can be estimated from the shift of the conformational equilibrium for such probes introduced into glassy polymers. If no conformational transitions occur at a certain temperature (conformational equilibrium is 'frozen'), the FVE size is less than the critical probe size necessary for its isomerisation. At certain temperature, the ratio of the conformers changes, which means that the FVE size at this temperature is comparable with the probe size. The experimentally used conformation probes were dichloroethane, 1,2-bromofluoroethane, 1,1,2,2-tetrabromoethane and some other compounds. Free-volume studies were carried out for polystyrene, poly(vinyl chloride), poly(methyl methacrylate) and some other glassy polymers. For each probe, the characteristic IR bands corresponding to *trans*- or *gauche*-conformations were chosen. At low temperatures, the optical density ratio D_{gauche}/D_{trans} is independent of temperature, then an inflection is observed at certain T_f value after which this ratio (in the $1/T$ coordinates) linearly decreases with temperature. Because the volume necessary for isomerisation of a given probe is known, one can estimate the FVE size at T_f. As the probe size increases, the T_f increases. This makes it possible to estimate the temperature dependence of the limiting FVE size ($V^{\neq}$) necessary for the conformational transition (isomerisation) of the probe in the polymer under study. An example of this dependence for poly(methyl methacrylate) is presented in Table 7. The results obtained are comparable with the PALS data.[143]

Table 7. Temperature dependence of FVE size in PMMA from the conformation probe technique data.[143]

Probe	T_f/K	$V^{\neq}$/Å^3
1-Bromo-2-fluoroethane	190 ± 20	13.0
1,2-Dichloroethane	195 ± 10	29.5
1,1,2,2-Tetrabromoethane	239 ± 9	56.6
1,2-Di(*p*-bromophenyl)ethane	326 ± 18	108.2

Experiments with the same probe in different polymers showed that for polymers with high permeabilities the conformational mobility of the probe unfreezes at much lower temperatures than for polymers with low permeabilities. For instance, T_f = 326 K for PMMA and 163 K for PTMSP with 1,2-di(*p*-bromophenyl)ethane as probe. Unfreezing of conformation transitions of a smaller probe (1,1,2,2-tetrabromoethane) in PTMSP occurs at even lower temperatures (T_f < 90 K).

However, this method is of limited use for studying the free volume in polymers due to the overlap of the spectral bands of the probe and polymer, scarcity of probes and problems associated with the introduction of the probe into the polymer from a common solvent.

On the whole, the methods considered in this Section cannot compete in reliability and informativity with the PALS technique. However, some of them played an important role in the early stage of development of studies on the free volume in polymers and still remain suitable for obtaining additional useful information.

VI. Simulation of the free volume by molecular dynamics

So far, we considered experimental methods of investigation of the free volume. Recently, methods of computer simulation of the nanostructure of polymers aimed at predicting many properties of

polymeric materials [in particular, the diffusion (D) and gas solubility (S) coefficients] have become increasingly important. When solving such problems, the construction of a correct model for the free volume in the polymer under study is prerequisite for obtaining accurate results. The results of computer simulation are analysed using relevant data obtained by probe techniques for substantiation of the reliability of calculations. At the same time, MD simulation provides valuable information that cannot be obtained by the probe methods (see below).

The free volume in polymers can be simulated by, *e.g.*, the Monte Carlo method,[8, 144–148] molecular mechanics,[8, 149, 150] theory of transition state and related approaches.[8, 151, 152] MD simulation appeared to be the most efficient method and a large number of polymers were studied by this method in recent years. In this Section we will consider the results of MD simulation of the free volume in amorphous polymers.

In MD simulation of amorphous polymers, the free volume is described using a cubic box filled with polymer chains. The results of analysis of the free volume and theoretical parameters including D and S can depend on the size of the cubic box, which is undesirable. Calculations with small boxes (cube edge is shorter than 20 Å) take a shorter time. Starting with a certain size (cube edge of about 40 – 50 Å) this correlation is no longer valid, but the results become more reliable. Usually, the model boxes contain 2000 to 10 000 atoms in the polymer chain.[153] All atoms in the polymer chains are represented by spheres of preset diameters and masses. The interactions of covalently bonded atoms are described with allowance for the bond lengths, bond angles and torsion angles. Non-covalent intermolecular interactions are described using commonly accepted (most often, the Lennard-Jones and Coulomb) potentials. The chemical structure of the polymer studied is determined in different approximations. The 'United Atoms' method ignores all hydrogen atoms and treats all quasi-spherical atomic groups (*e.g.*, CH_2, CH_3) as individual species in order to reduce the computing time. More reliable results can be obtained using the 'All-Atom Strategy'.[11]

The sum of all atom – atom interactions expressed as the potential energy model of the packing is called the force field. A correctly determined force field is the key for successful MD simulation of the nanostructure of the system. The force field should reproduce the equilibrium structure, thermodynamic and dynamic properties of the polymer under study and govern the accuracy of prediction of all parameters of the system. One of the most popular force field types is known as the COMPASS (Condensed-phase Optimized Molecular Potentials for Atomistic Simulation Studies) [154] force field (for details, see Ref. 8).

Theodorou and Suter [155, 156] proposed an efficient box-filling procedure, which allows the length of the polymer chain to be chosen in such a manner that the packing be completely amorphous. The polymer chains are generated using the so-called periodic boundary conditions. Namely, as a propagating virtual chain reaches a cube face and starts to 'penetrate' it, a similar propagating chain is automatically introduced on the opposite face. The box is filled until a preset, experimentally determined density of the polymer is reached. Therefore, the polymer density serves as an 'input parameter' for calculations. This can cause some difficulties, because the densities of glassy polymers depend on the sample prehistory, amount of residual solvent, *etc*. Since the number of possible types of packing within the cubic box is infinitely large, a packing containing domains with too low or too high local density can be formed in the initial stage. Obtaining a more realistic packing requires an additional stage of the process, namely, the relaxation stage. Various procedures are used to accelerate relaxation. In particular, molecules of 'plasticiser' (*e.g.*, methanol) can be introduced into the box and then removed upon relaxation. Detailed consideration of the polymer structure models can be found in, *e.g.*, Refs 8, 111, 153, 157 and 158.

Computer simulation opens new, additional prospects for investigation of the free volume in polymers, most of which are inaccessible in principle to probe methods:

— visualisation of the free volume;

— analysis of connectivity of free-volume elements (cluster size, closed or open porosity);

— construction of FVE size distribution;

— studies of mobility (dynamics) of the free volume elements in polymers.

Consider as an example model nanostructures of the free volume [111, 157] in a polymer with moderate permeability, poly(*p*-trimethylsilylstyrene) (P_{O_2} = 56 Barrer [159]) and in two polymers with high permeabilities and large FVE (according to PALS and IGC data), namely, poly(trimethylsilylpropyne) and amorphous Teflon AF2400 (P_{O_2} = 7700 and 1140 Barrer, respectively [41, 160]). The force field was calculated using the COMPASS programme,[154] which includes interactions of all atoms in the monomer unit in explicit form and optimizes the bond lengths, bond angles, dihedral angles and the Coulomb and van der Waals potentials. Calculations involve optimisation of the force field in order to correctly reproduce the physical properties of the polymer in the block. The *cis* : *trans* ratio in PTMSP, which contains double bonds in the main chain, was set to 1 : 1 assuming random distribution of *cis* and *trans* units over the chain. In this approximation all dihedral angles were determined based on the Boltzmann distribution obtained using the torsion potentials included in the COMPASS force field for particular bonds with allowance for local non-bonding interactions.

It is convenient to carry out visualisation by slicing the cubic boxes generated. In boxes with 4 – 5 nm edges, the neighbouring layers are separated by a distance of about 0.3 nm (Fig. 7). In Fig. 7 *a*, the white background denotes the free volume; the free volume elements in PTMSS represent compact aggregates the size of which is comparable with the slice-to-slice separation. For instance, the visible FVE in slice c_4 is not seen in the neighbouring slices c_3 and d_1. This means that the FVE size is comparable with the slice-to-slice separation of $\sim$0.3 nm. The visible 'diameter' of FVE in this slice is also similar to this value. Thus, our simplest analysis shows that the shape of the free volume elements in PTMSS is nearly spherical or ellipsoidal with similar lengths of semiaxes. PTMSP has another shape of the free volume elements (Fig. 7 *b*). Here, the characteristic size of FVE is much larger and the same FVE can be seen in many slice sequences in the cubic box. This can be considered as a proof of the assumptions of quasi-open porosity in this polymer, which were based on some indirect observations.[161, 162] A broad FVE size distribution was also obtained in another study [152] where it was found that larger FVE tend to form channels.

According to MD simulation data, the other polymer with high permeability, *viz*., amorphous Teflon AF2400, has yet another type of the nanostructure of the free volume elements. The results of MD simulation of the packing in this polymer showed [111] that the FVE size here is also rather large, but the FVE no longer pierce the whole cubic box, as in the case of PTMSP. Elongated FVE rarely extend to more than one or two slices. Thus, the structure of the AF2400 polymer is rather characterised by the closed porosity.

It is interesting to follow how these microscopic properties are reflected in the macroscopic behaviour of membrane materials, in particular their gas permeabilities and diffusion coefficients (Table 8). Since

$$P = DS,$$

the changes in P in series of penetrants are governed by the kinetic (D) or thermodynamic (S) factors. For all polymers their D values decrease, although at different rates, as the size or molecular mass of penetrant increase. On the contrary, the solubility coefficients S, which characterise the ability of transition to condensed state,

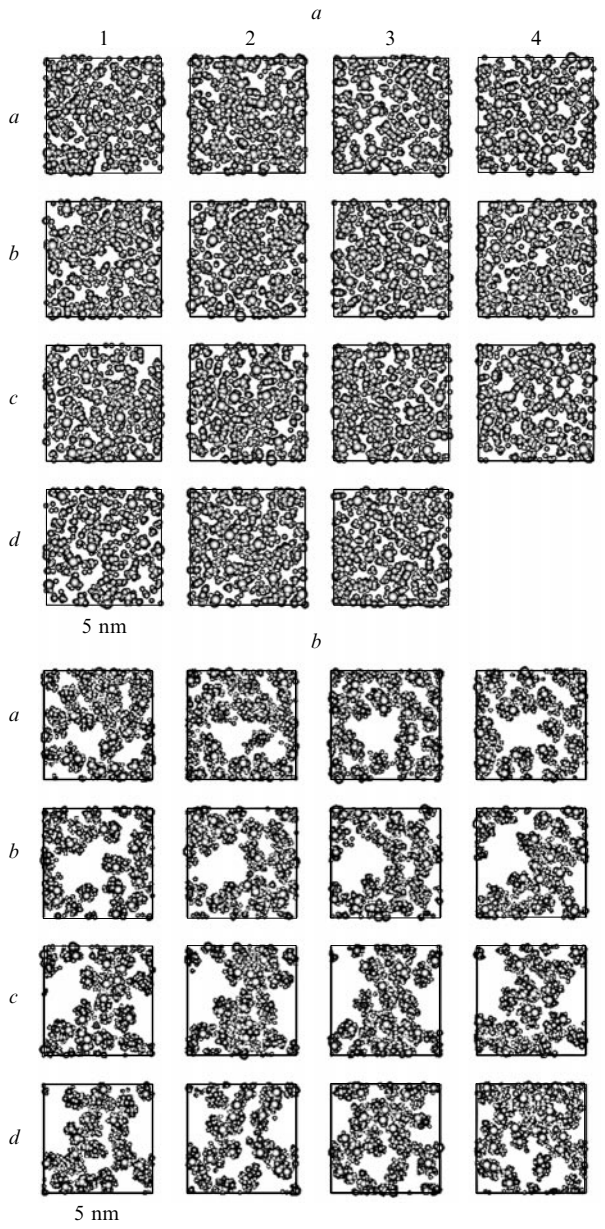


Figure 7. Model representation of the free volume in PTMSS (*a*) and PTMSP (*b*).[157]
Cube edge is about 5 nm, slice-to-slice separation is nearly 0.3 nm; slices are shown as follows: $a_1 \ldots a_4$, $b_1 \ldots b_4$, $c_1 \ldots c_4$, $d_1 \ldots d_3(d_4)$.

Table 8. Permeability and diffusion coefficients of hydrocarbons in AF2400 and PTMSP.

Gas	P /Barrer		$10^7 D$ /cm^2 s^{-1}	
	AF2400 [41]	PTMSP [163]	AF2400 [41]	PTMSP [163]
CH_4	435	15 000	–	240
C_2H_6	252	31 000	3.6	110
C_3H_8	97	38 000	0.42	98
C_4H_{10}	–	78 000 [a]	0.24	–

[a] Data taken from Ref. 162.

increase in this case. In polymers the with open porosity characterised by low barriers to diffusion the parameter P is more strongly affected by the solubility coefficient S. It is this behaviour that is typical of PTMSP, which has a relatively weak dependence of D on the size of the penetrant. Contrary to this, polymer AF2400 behaves as a conventional glassy polymer and demonstrates a rather strong dependence of D on the size of the penetrant; therefore, here the P values decrease on going from CH_4 to C_3H_8. Thus, the connectivity of the free volume elements has a crucial effect on the selectivity of glassy membrane materials.

Using MD simulation, it is possible to determine the FVE size distribution. The corresponding procedure involves filling of the box with probes of different size and calculations of the volume where the rigid spheres of the probes and polymer atoms do not overlap. However, because the free volume in polymers has a complex geometry (irregular shape; for details, see, *e.g.*, Refs 164–167), the results obtained can depend on how the notion 'FVE' used in analysis of the computer model is defined. Hofmann *et al.*[111, 157, 168] put forward two definitions of the FVE in polymers; these are illustrated in Fig. 8. One limiting case (V_connect approximation) corresponds to a topological situation where a given FVE contains all points having at least one neighbour with no overlap of the rigid spheres of the probe and atoms of the polymer chain. This approach makes it possible to identify cavities that can be large and have irregular shape. In the other limiting case (R_max approximation), the FVE contains only the points located at the shortest distance to the atoms of the polymer chain surrounding the FVE. This approach allows partition of large FVE having irregular or extended shape into smaller 'local' regions, as shown in Fig. 8.

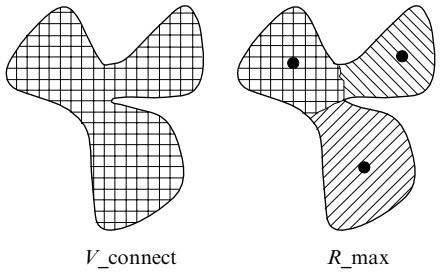


Figure 8. Schematic illustration of two approaches to visualisation of the free volume in glassy polymers.[157]
The V_connect approximation characterises the 'global' FVE, while the R_max approximation characterises the 'fractional' FVE more similar to spherical.

Now consider how the shape of the FVE size distribution in polymers, obtained using these two approximations, are represented. PTMSS is characterised by a nearly Gaussian distribution with a maximum at $R = 2$ Å (Fig. 9), which is consistent with the results of qualitative analysis of the cubic box (see above and Fig. 7 *a*). For this polymer, both approximations give similar FVE size distributions. Another pattern was obtained for the polymers with high permeabilities and large free volumes. As examples, Fig. 10 presents the FVE size distributions obtained for amorphous Teflon AF2400 in the R_max and V_connect approximations. In the former case, this is a broadened continuous FVE size distribution with radii of up to 13 Å. In the latter case, we have a clearly seen bimodal distribution consistent with the results of PALS data processing using the CONTIN programme (see Section II). Because the real structure of the free volume in polymers should be considered as superposition of these two limiting models, it seems that we get even better agreement between the predictions of MD simulations and experimental results obtained using probe methods.

Similar characters of the distributions obtained in the V_connect and R_max approximations were also established for PTMSP

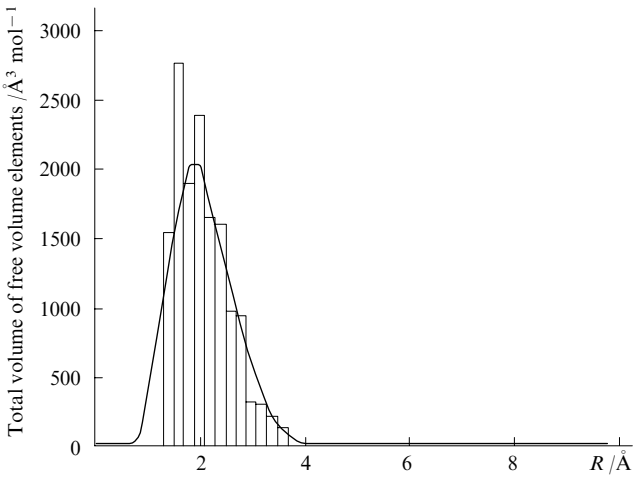


Figure 9. Size distribution of free volume elements in PTMSS.[157]
Rectangles denote the results obtained in the *R*_max approximation. The curve corresponds to averaged data.

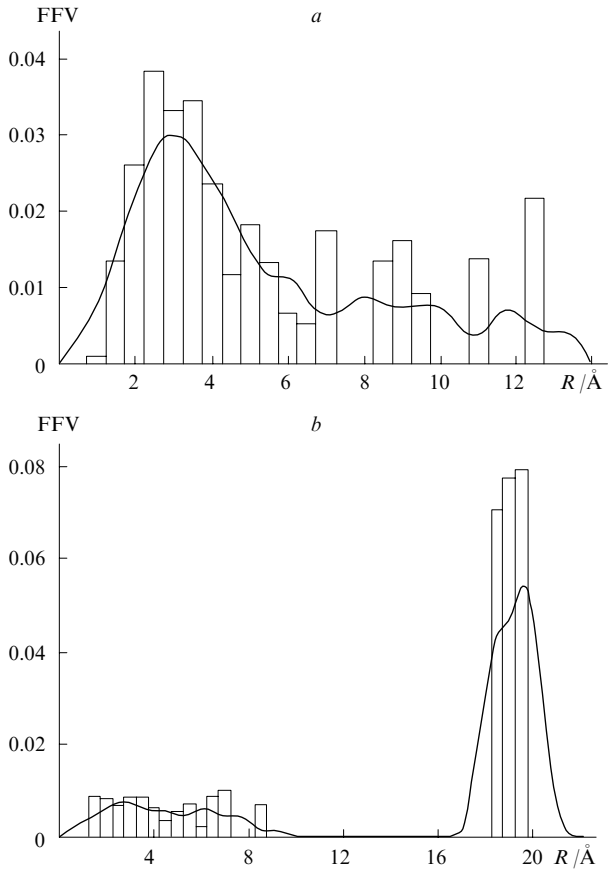


Figure 10. Size distribution of free volume elements in perfluorinated polymer AF2400.[111]
Results obtained in the *R*_max (*a*) and V_connect (*b*) approximations. Rectangles denote the corresponding theoretical results and the curves correspond to averaged data.

and other polymers with high permeabilities.[111] Bimodal distributions in the *V*_connect approximation were also obtained in simulation of polymers with smaller permeabilities (polyimides, see Fig. 11). However, a decrease in gas permeability (and free volume) of polyimides is followed by rapid transformation of the bimodal distribution to monomodal (Gaussian).[168]

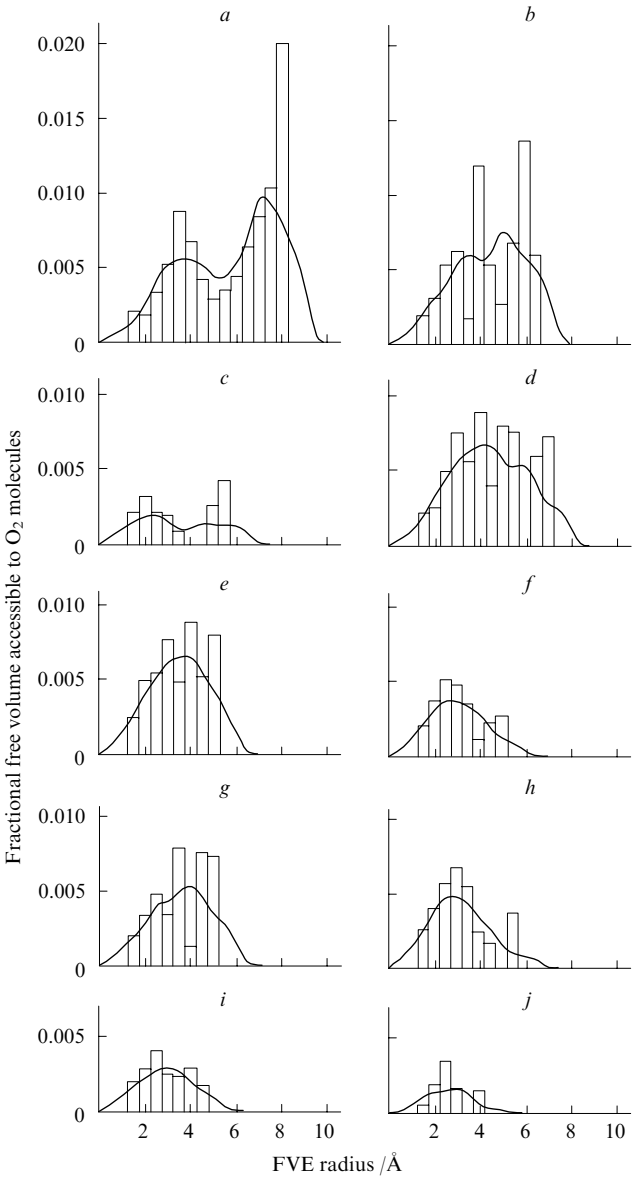


Figure 11. Size distribution of free volume elements in different polyimides.[168]
Shown is the evolution of the size distribution upon a change in the polymer permeability P_{O_2} /Barrer: P13, $P_{O_2} = 124$ (*a*); P14, $P_{O_2} = 137$ (*b*); T6, $P_{O_2} = 69$ (*c*); B4, $P_{O_2} = 54$ (*d*); BAFF, $P_{O_2} = 13$ (*e*); MDX, $P_{O_2} = 11$ (*f*); PDA, $P_{O_2} = 5$ (*g*); ODX, $P_{O_2} = 4$ (*h*); DDS, $P_{O_2} = 3$ (*i*); and KAP, $P_{O_2} = 0.5$ (*j*).

The character of the FVE size distribution depends on the probe size. For instance, the use of oxygen molecules (van der Waals radius 1.73 Å) instead of *o*-Ps (Bohr radius 1.06 Å) as probes causes the distribution to be shifted to the left at larger radii; however, the overall distinctions between the two distributions are insignificant.[111]

By substantially reducing the probe size, one can plot the 'total' FVE size distribution [157, 169] (Table 9), which includes even so small cavities that cannot participate in transport of the smallest molecules. For most glassy polymers extrapolation to zero probe size gives a FFV of about 0.3, but in some cases (*e.g.*, PTMSP) it can be as high as 0.5 (Ref. 157). Taking atactic polypropylene as an example, Greenfield and Theodorou [144] showed that a decrease in the probe size causes a rapid increase in continuous free-volume clusters in the polymer, which overcome the percolation threshold. Indeed, an infinite cluster is

Table 9. FFV estimates obtained from MD simulation with probes of different sizes.[157]

Polymer	Probe size /Å	FFV
PTMSS	1.1	0.02
	0.43	0.185
	0.18	0.331
	extrapolation to zero	~0.36
PTMSP	1.1	0.211
	0.43	0.369
	0.18	0.469
	extrapolation to zero	~0.50

formed at a virtual (unnatural) probe radius of 0.9 Å (*cf.* a range from 1.20 to 1.30 Å reported by different authors for the van der Waals radius of the He atom).

Correctness of the results of MD simulation of the free volume in polymers can be assessed not only by comparing them with the results obtained by experimental probe methods, but also by checking for consistence with the FVE size distributions in the same polymers treated using different computational approaches (see, *e.g.*, Refs 157 and 169). To date, MD simulations of the free volume in many glassy polymers (polyimides, polysulfones, polystyrenes, polyacetylenes, *etc.*) have been carried out.[110, 148, 160, 163, 164] For most polymers, the FVE radii lie in the range 2–4 Å, which is consistent with the data obtained by two probe methods, PALS and ^{129}Xe NMR spectroscopy. However, for some polymers with high permeabilities MD simulation gives much larger FVE radii (up to 10–20 Å), which undoubtedly determines unusual transport properties of these compounds. Selected results of MD simulation of the free volume and experimental PALS data are listed in Table 10. Taking into account a large number of admissions made in both MD simulation and experimental free-volume studies, the degree of consistency obtained for most polymers can be considered reasonable.

In the aforesaid we considered the static free volume in polymers. However, MD methods are also suitable for studying the redistribution dynamics of FVE in polymers. For rubbers [*e.g.*, polydimethylsiloxane, poly(methyloctylsiloxane)[172–174] and poly(dimethylsilamethylene)[158]] the average lifetime of FVE in a certain domain within the box is a few picoseconds while the opening of channels connecting the neighbouring FVE seems to take even shorter time. Glassy polymers, *e.g.*, polyimides and poly(ether-ether-ketone)[172, 175] are characterised by much longer average lifetimes, but reliable data on these times are unavailable as yet, because analysis of the events occurring on a few-nanosecond time scale requires unreasonably high computational resources.

The time necessary for visualisation of FVE redistribution in glassy polymers is much longer than several nanoseconds.[158]

Consider the dynamics of FVE redistribution in rubbers[153, 158, 172] in more detail. Simulation of the free volume in poly(methyloctylsiloxane) rubber showed that the opening time of a channel between neighbouring FVE is of the order of nanoseconds, *i.e.*, is two orders of magnitude longer than the 'settled' lifetime of the penetrant molecule (H_2O). Channels being opened are rather broad; as a result, two neighbouring FVE coalesce. This provides an explanation for the well-known phenomenon of low-selectivity diffusion in rubbers; indeed, here size selection of the diffusing molecules in the opening channels is impossible. Microscopically, migration of FVE (or, which is the same, opening of channels) is a consequence of both segmental mobility and small-scale mobility of side groups (CH_3 and C_8H_{17} for poly(dimethylsiloxane) and poly(methyloctylsiloxane),[153] respectively).

Table 10. FVE radii (Å) in polymers obtained from molecular dynamics simulation and by PALS.

Polymer	MD simulation			PALS			
	R_m	$R_{1/2}$	Ref.	R	R_3	R_4	Ref.
6FDA-polyimides							
P13	3.0	1.3–4.5	168	4.2			76
P14	2.7	1.4–4.4	168	4.0			76
BAAF	2.7	1.3–4.0	168	3.6			76
	2.7	1.3–3.7	170				
PDA	2.6	1.3–4.0	168	3.4			76
ODA	2.6	1.3–3.8	168	3.2			76
PS	3.2	2.9–3.6	167	2.7; 2.9			33 171
PTMSS	1.9	1.3–2.8	157		2.6	3.8	159
PFPDMSS	1.8	1.3–2.6	157	3.6			157
PSP	1.2	0.8–2.2	170	2.8			34, 172
PVTMS	2.6	1.3–4.4	111	3.4			111
PTMSP	4.5	1.7–8.0	111		3.3	6.3	111, 157
	5.6	4.7–7.4	169				
PPrSiDPA	3.1	1.3–4.9	111		4.4	6.5	111
PPHSiDPA	2.7	1.0–4.7	111		2.6	4.1	111
AF2400	4.7	3.3–5.5	169		2.7	6.0	111
AF1600	3.1	1.6–5.2	111		2.5	4.9	111
						4.8	40

Note. R_m is the FVE radius at the distribution maximum; the width of the FVE size distribution is represented by the range of $R_{1/2}$ (radii at half-height) values; PALS data are represented by either a unique radius of spherical FVE (R) or two values (R_3 and R_4) if the size distribution is bimodal.

Similar conclusions were also drawn in studies of the dynamics of fluctuating FVE in another organosilicon rubber, poly(dimethylsilamethylene).[158] MD simulation of this polymer was carried out for the free volume 'sensed' by two penetrant molecules of different sizes, namely, methane and a spherical penetrant with diameter of 2.8 Å (similar to the size of H_2 molecule). The FVE concentrations accessible to methane molecule appeared to be much lower than those accessible to the smaller penetrant. In both cases the larger FVE were characterised by longer 'settled' lifetimes compared to the smaller FVE. The spatial FVE distribution significantly changed after a period of 10 ns (time interval between two successive 'frames' in MD simulation of the free-volume dynamics); the effective diffusion coefficients of FVE were of the order of 10^{-3}–10^{-4} cm s^{-1}. This provides an explanation for fast gas diffusion in rubbers.

VII. Conclusion

At present, the free volume in polymers is studied by experimental methods based on different physicochemical principles and measuring techniques. On the whole these techniques give mutually consistent results. Among them, analysis of positron annihilation lifetimes has been best developed and most often used. Despite some admissions associated with uncertainties in the hypothesis of spherical geometry of the FVE in polymers and some doubt concerned with bimodal FVE size distribution, this method gave a clear description of the free volume in hundreds of polymers. Also, it is at least equally important that the method makes it possible to study changes in the free volume upon chemical modification of polymers, sorption and plastification, upon change in temperature and under the action of pressure and deformations.

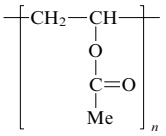
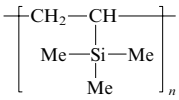
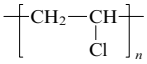
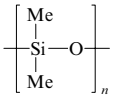
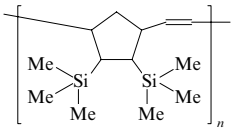
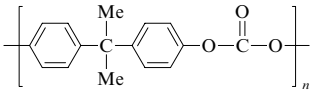
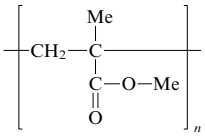
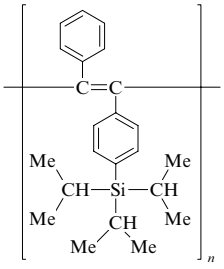
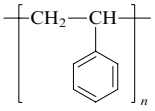
The results obtained showed that other probe methods are of much more limited use. However, their role should not be under-

estimated. Indeed, reasonable agreement between the FVE sizes determined by different methods increases the degree of confidence for the principle of probing the free volume in polymers. This made it possible to establish various correlations between the free volume and particular characteristics (*e.g.*, diffusion coefficients and gas permeabilities), which are suitable for quantitative predictions.

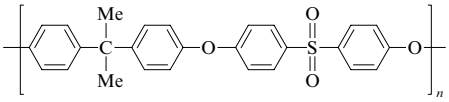
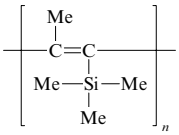
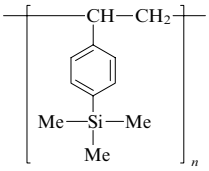
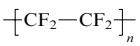
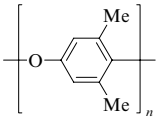
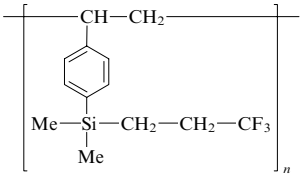
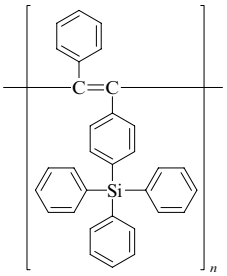
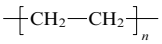
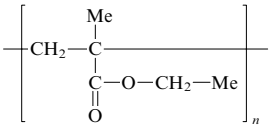
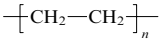
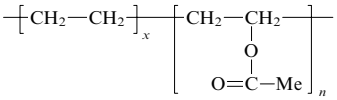
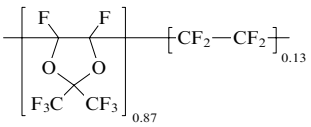
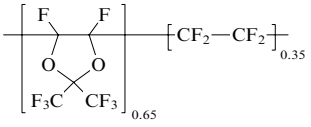
Recently, MD methods have become of particular importance for the description and prediction of free-volume parameters. The results obtained by the probe methods are still needed to confirm the results of simulation, but it seems likely that in the future the MD methods will become the main tool of studying the free volume in polymers. It is also of crucial importance that MD simulation provides not only local characteristics of the free volume (FVE size and FVE size distribution), but also information on its topology (closed or open porosity, percolation phenomena, *etc.*). This is inaccessible to probe methods. The aforesaid suggests that the results of studies on the properties of polymers (*e.g.*, membrane polymers) should be complemented with the data obtained by probe methods and by the results of MD simulation of the free volume in polymers.

VIII. Appendix

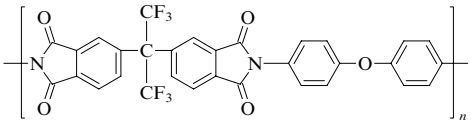
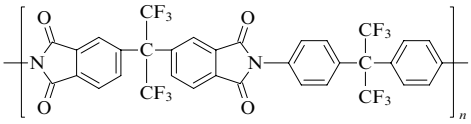
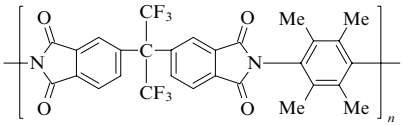
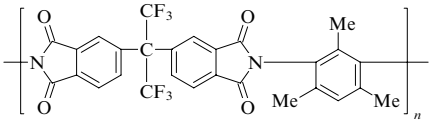
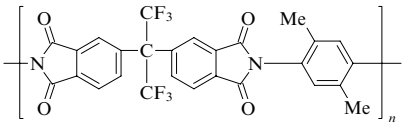
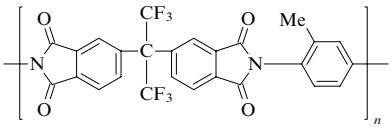
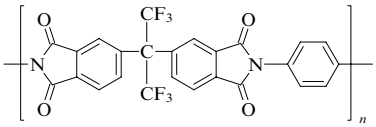
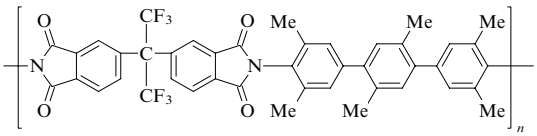
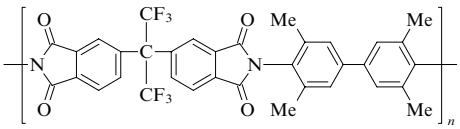
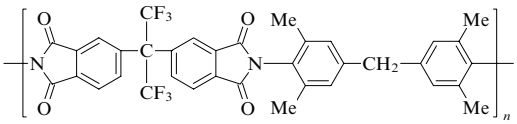
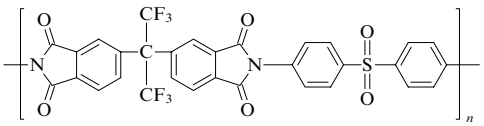
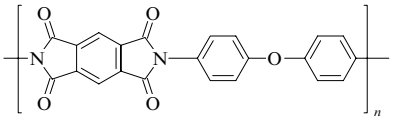
List of polymers.

Notation	Name	Formula
PVA	poly(vinyl acetate)	
PVTMS	poly(vinyltrimethylsilane)	
PVC	poly(vinyl chloride)	
PDMS	poly(dimethylsiloxane)	
PDSNb	poly(disilylnorbornene)	
PC	bisphenol-A polycarbonate	
PMMA	poly(methyl methacrylate)	
PPrSiDPA	poly{1-phenyl-2-[*p*-(triisopropylsilyl)phenyl]}acetylene	
PS	polystyrene	

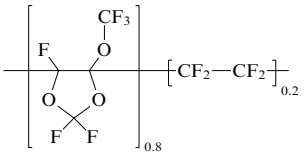
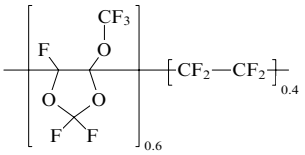
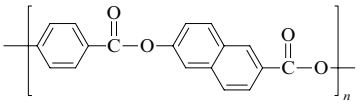
List of polymers (continued).

Notation	Name	Formula
PSP	polysulfone	
PTMSP	poly(trimethylsilylpropyne)	
PTMSS	poly(*p*-trimethylsilylstyrene)	
PTFE	poly(tetrafluoroethylene)	
PPO	poly(1,3-dimethyl-2,5-phenylene oxide)	
PFPDMSS	poly[*p*-(3,3,3-trifluoropropyl)dimethylsilyl]styrene	
PPHSiDPA	poly{1-phenyl-2-[*p*-(triphenylsilyl)phenyl]}acetylene	
PE	polyethylene	
PEMA	poly(ethyl methacrylate)	
LDPE	low-density polyethylene	
EVA	ethylene – vinyl acetate copolymer	
AF-2400	random copolymer of 2,2-bis(trifluoromethyl)-4,5-difluoro-1,3-dioxole (87 mol.%) and tetrafluoroethylene (13 mol.%)	
AF-1600	random copolymer of 2,2-bis(trifluoromethyl)-4,5-difluoro-1,3-dioxole (65 mol.%) and tetrafluoroethylene (35 mol.%)	

List of polymers (continued).

Notation	Name	Formula
6FDA-ODA	polyimide based on 1,1,1,3,3,3-hexafluoro-2,2-bis(3,4-dicarboxyphenyl)propane dianhydride and 4,4′-diaminodiphenyl ether	
6FDA-BAAF	polyimide based on 1,1,1,3,3,3-hexafluoro-2,2-bis(3,4-dicarboxyphenyl)propane dianhydride and 2,2-bis(4-aminophenyl)hexafluoropropane	
6FDA-P13	polyimide based on 1,1,1,3,3,3-hexafluoro-2,2-bis(3,4-dicarboxyphenyl)propane and 2,3,5,6-tetramethyl-*p*-phenylenediamine	
6FDA-P14	polyimide based on 1,1,1,3,3,3-hexafluoro-2,2-bis(3,4-dicarboxyphenyl)propane dianhydride and 2,4,6-trimethyl-*m*-phenylenediamine	
6FDA-2	polyimide based on 1,1,1,3,3,3-hexafluoro-2,2-bis(3,4-dicarboxyphenyl)propane dianhydride and 2,5-dimethyl-*p*-phenylenediamine	
6FDA-1	polyimide based on 1,1,1,3,3,3-hexafluoro-2,2-bis(3,4-dicarboxyphenyl)propane dianhydride and methyl-*p*-phenylenediamine	
6FDA-PDA	polyimide based on 1,1,1,3,3,3-hexafluoro-2,2-bis(3,4-dicarboxyphenyl)propane dianhydride and *p*-phenylenediamine	
6FDA-T6	polyimide based on 1,1,1,3,3,3-hexafluoro-2,2-bis(3,4-dicarboxyphenyl)propane dianhydride and 4,4″-diamino-3,5,2′,5′,3″,5″-hexamethylterphenyl	
6FDA-B4	polyimide based on 1,1,1,3,3,3-hexafluoro-2,2-bis(3,4-dicarboxyphenyl)propane dianhydride and 4,4′-diamino-3,5,3′,5′-tetramethylbiphenyl	
6FDA-MDX	polyimide based on 1,1,1,3,3,3-hexafluoro-2,2-bis(3,4-dicarboxyphenyl)propane dianhydride and 4,4′-diamino-3,5,3′,5′-tetramethyldiphenylmethane	
DDS	polyimide based on 1,1,1,3,3,3-hexafluoro-2,2-bis(3,4-dicarboxyphenyl)propane dianhydride and 4,4′-diaminodiphenyl sulfone	
KAP	polyimide of pyromellitic dianhydride and 4,4′-diaminodiphenyl oxide	

List of polymers (continued).

Notation	Name	Formula
Hyflon AD80X	random copolymer of 2,2,4-trifluoro-5-trifluoromethoxy-1,3-dioxolane (80 mol.%) and tetrafluoroethylene (20 mol.%)	
Hyflon AD60X	random copolymer of 2,2,4-trifluoro-5-trifluoromethoxy-1,3-dioxolane (60 mol.%) and tetrafluoroethylene (40 mol.%)	
Vectra	copolyester of *p*-hydroxybenzoic acid and 6-hydroxy-2-naphthoic acid	

References

1. Ya I Frenkel' *Sobranie Izbrannykh Trudov. Kineticheskaya Teoriya Zhidkostei* (Collected Selected Works. Kinetic Theory of Liquids) (Moscow, Leningrad: Academy of Sciences of the USSR, 1959) Vol. 3
2. M H Cohen, D Turnbull *J. Chem. Phys.* **31** 1164 (1959)
3. D Turnbull, M H Cohen *J. Chem. Phys.* **34** 120 (1961)
4. J S Vrentas, J L Duda, in *Encyclopedia of Polymer Science and Engineering* Vol. 5 (New York: Wiley, 1986) p. 36
5. J L Duda, J M Zelinsky *Free-Volume Theory in Diffusion in Polymers* (Ed. P Neogi) (New York: Marcel Decker, 1996)
6. A A Askadskii, Yu I Matveev *Khimicheskoe Stroenie i Fizicheskie Svoistva Polimerov* (Chemical Structure and Physical Properties of Polymers) (Moscow: Khimiya, 1983)
7. A A Askadskii, V I Kondrashchenko, in *Komp'yuternoe Materialovedenie Polimerov. Atomno-molekulyarnyi Uroven'* (Computer Materials Science of Polymers. Atomic-molecular Level) (Moscow: Nauchnyi Mir, 1999) Vol. 1, p. 54
8. A Bondi *Physical Properties of Molecular Crystals, Liquids and Gases* (New York: Wiley, 1968)
9. J Y Park, D R Paul *J. Membr. Sci.* **125** 23 (1997)
10. D N Theodorou, in *Molecular Simulations of Sorbtion and Diffusion in Amorphous Polymers in Diffusion in Polymers* (Ed. P Neogi) (New York: Marcel Decker, 1996) p. 67
11. D N Theodorou, in *Principles of Molecular Simulation of Gas Transport in Polymers. (Materials Science of Membranes for Gas and Vapour Separation)* (Eds Yu Yampolskii, I Pinnau, B D Freeman) (New York: Wiley, 2006) p. 47
12. D M Shrader, Y C Jean (Eds) *Positron and Positronium Chemistry* (Amsterdam: Elsevier, 1988)
13. R A Pethrick *Prog. Polym. Sci.* **22** 1 (1997)
14. A Hill, in *High Temperature Properties and Applications of Polymeric Materials (ACS Symp. Ser.)* (Eds M R Tant, J W Connell, H L N McManus). (Washington, DC: American Chemical Society, 1995) Vol. 603, p. 63
15. J Bartos, in *Encyclopedia of Analytical Chemistry* (Ed. R A Meyers) (New York: Wiley, 2000) p. 7968
16. M Ban, M Kyoto, A Uedono, T Kawano, S Tanigawa *J. Polym. Sci., Part B: Polym. Phys.* **34** 1189 (1996)
17. C Westlund, M Eldrup, F H J Maurer *Nucl. Instrum. Methods Phys. Res., Sect. B* **143** 575 (1998)
18. W Brandt, J Spirn *Phys. Rev.* **142** 231 (1966)
19. J Tao *J. Chem. Phys.* **56** 5499 (1972)
20. M Eldrup, D Lightbody, J N Sherwood *Chem. Phys.* **63** 51 (1981)
21. A Shimazu, T Miyazaki, S Katayama, Y Ito *J. Polym. Sci., Part B: Polym. Phys.* **41** 308 (2003)
22. P Kirkegaard, N J Pederson, M Eldrup *PATFIT-88: A Data Processing System for Positron Annihilation Spectra on Mainframe and Personal Computers, Roskilde, Denmark, 1989* Risoe-M-2740
23. S W Provencher *Comput. Phys. Commun.* **27** 229 (1982)
24. R B Gregory *J. Appl. Phys.* **70** 4665 (1991)
25. C-L Wang, F H J Maurer *Macromolecules* **29** 8249 (1996)
26. B Nagasaka, T Eguchi, H Nakayama, N Nakamura, Y Ito *Radiat. Phys. Chem.* **58** 581 (2000)
27. B G Olson, T Prodpran, A M Jamieson, S Nazarenko *Polymer* **43** 6775 (2002)
28. Y C Jean, H Shi *J. Non-Cryst. Solids* **172–174** 806 (1994)
29. T Goworek, K Ciesielski, B Jasinska, J Wawzyszuk *Radiat. Phys. Chem.* **58** 719 (2000)
30. T Hsieh, C Tiu, G P Simon *J. Appl. Polym. Sci.* **82** 2252 (2001)
31. V P Shantarovich, Yu P Yampolskii, Yu M Sivergin, O B Salamatina, V V Gustov, D Khofmann *Khim. Fiz.* **22** 87 (2003) [a]
32. J Liu, Q Deng, Y C Jean *Macromolecules* **26** 7149 (1993)
33. Y C Jean, J-P Yuan, J Liu, Q Deng, H Yang *J. Polym. Sci., Part B: Polym. Phys.* **33** 2365 (1995)
34. K Tanaka, K Okamoto, H Kita, Y Ito *Polym. J. (Tokyo)* **25** 577 (1993)
35. V Shantarovich, I Kevdina, Yu Yampolskii, A Alentiev *Macromolecules* **33** 7453 (2000)
36. A Shimazu, T Kanaya, T Miyazaki, S Katayama, Y Ito *Mater. Sci. Forum* **445–446** 249 (2004)
37. K Okamoto, K Tanaka, M Ito, H Kita, Y Ito *Mater. Sci. Forum* **175–178** 743 (1995)
38. V Shantarovich, Z Azamatova, Yu Novikov, Yu Yampolskii *Macromolecules* **31** 3963 (1998)
39. G Consolati, I Genco, M Pegoraro, L Zanderighi *J. Polym. Sci., Part B: Polym. Phys.* **34** 357 (1996)
40. W J Davies, R A Pethrick *Eur. Polym. J.* **30** 1289 (1994)
41. A Yu Alentiev, Yu P Yampolskii, V P Shantarovich, S M Nemser, N A Plate *J. Membr. Sci.* **126** 123 (1997)
42. G Consolati, R Rurali, M Stefanetti *Chem. Phys.* **237** 493 (1998)
43. V P Shantarovich, T Suzuki, C He, V A Davankov, A V Pastukhov, M P Tsyurupa, K Kondo, Y Ito *Macromolecules* **35** 9723 (2002)
44. V P Shantarovich, T Suzuki, C He, I B Kevdina, V A Davankov, A V Pastukhov, M P Tsuryupa *High Energy Chem.* **38** 274 (2004)
45. G Ferey, C Mellot-Draznieks, C Serre, F Millange, J Dutour, S Surble, I Margiolaki *Science* **309** 2040 (2005)
46. N B McKeown, S Makhseed, K J Msayib, L L Ooi, M Helliwell, J E Warren *Angew. Chem., Int. Ed.* **44** 7718 (2005)

47. Y Kobayashi, W Zheng, E F Meyer, J D McGervey, A M Jamieson, R Simha *Macromolecules* **22** 2302 (1989)
48. Y Y Wang, H Nakanishi, Y C Jean, T C Sandreczki *J. Polym. Sci., Part B: Polym. Phys.* **28** 1431 (1990)
49. V Shantarovich, T Suzuki, C He, Y Ito, Yu Yampolskii, A Alentiev *Radiat. Phys. Chem.* **73** 45 (2005)
50. J Kristiak, J Bartos, K Kristiakova, O Sausa, P Bandzuch *Phys. Rev. B* **49** 6601 (1994)
51. H A Christov, B Bolan, A F Yee, L Xie, D W Gidley *Macromolecules* **29** 8507 (1996)
52. R Srithawatpong, Z L Peng, B G Olson, A M Jamieson, R Simha, J D McGervey, T R Meier, A F Halasa, H Ishida *J. Polym. Sci., Part B: Polym. Phys.* **37** 2754 (1999)
53. G Dlubek, K Saarinen, H M Fretwell *J. Polym. Sci., Part B: Polym. Phys.* **36** 1513 (1998)
54. G Dlubek, V Bondarenko, J Pionteck, M Supej, A Wutzler, R Krause-Rehberg *Polymer* **44** 1921 (2003)
55. J Bohlen, J Wolff, R Kirchheim *Macromolecules* **32** 3766 (1999)
56. S S Jordan, W J Koros *Macromolecules* **28** 2228 (1995)
57. V P Shantarovich *J. Radioanal. Nucl. Chem.* **210** 357 (1996)
58. V P Shantarovich, V I Goldanskii *Hyperfine Interact.* **116** 67 (1998)
59. G Dlubek, J Stejny, T Lüpke, D Bamford, K Peters, C Hubner, M A Alam, M J Hill *J. Polym. Sci., Part B: Polym. Phys.* **40** 65 (2002)
60. A Alentiev, Yu Yampolskii *J. Membr. Sci.* **206** 291 (2002)
61. G Dlubek, D Bamford, A Rodriguez-Gonzalez, S Bornemann, J Stejny, B Schade, M A Alam, M Arnold *J. Polym. Sci., Part B: Polym. Phys.* **40** 434 (2002)
62. G Dlubek, T Lüpke, J Stejny, M A Alam, M Arnold *Macromolecules* **33** 990 (2000)
63. J L Keddie, R A L Jones, R A Cory *Europhys. Lett.* **27** 59 (1994)
64. J A Forrest, K Dalnoki-Veress, J R Stevens, J R Dutcher *Phys. Rev. Lett.* **77** 2002 (1996)
65. B A Rozenberg, V I Irzhak, L M Bogdanova *Prog. Colloid Polym. Sci.* **80** 187 (1989)
66. S M Shishatskii, Yu P Yampolskii, K-V Peinemann *J. Membr. Sci.* **112** 275 (1996)
67. A L Volynskii, N F Bakeev *Vysokomol. Soedin., Ser. B* **45** 1209 (2003) [b]
68. D Schodbauer, G Kögel, P Sperr, W Triftshauser *Phys. Status Solidi A* **102** 549 (1987)
69. Y C Jean, H Cao, G H Dai, R Suzuki, T Ohdaira, Y Kobayashi, K Hirata *Appl. Surf. Sci.* **116** 251 (1997)
70. H Cao, J-P Yuan, R Zhang, C S Sundar, Y C Jean, R Suzuki, T Ohdaira, B Nielsen *Appl. Surf. Sci.* **149** 116 (1999)
71. J Algers, PhD Thesis, Lund University, Sweden, 2004
72. J Algers, R Suzuki, T Ohdaira, F H J Maurer *Macromolecules* **37** 4201 (2004)
73. J Algers, R Suzuki, T Ohdaira, F H J Maurer *Polymer* **45** 4533 (2004)
74. Yu P Yampolskii, E Sh Finkel'shtein, K L Makovetskii, I Ya Ostrovskaya, E B Portnykh, M L Gringol'ts, Yu G Ishutina, I B Kevdina, V P Shantarovich *Vysokomol. Soedin., Ser. A* **38** 1480 (1996) [b]
75. Yu P Yampolskii, E Sh Finkelshtein, K L Makovetskii, V I Bondar, V P Shantarovich *J. Appl. Polym. Sci.* **62** 349 (1996)
76. K Tanaka, M Katsube, K Okamoto, H Kita, O Sueoka, Y Ito *Bull. Chem. Soc. Jpn.* **65** 1891 (1992)
77. K Hagiwara, T Ougizawa, T Inoue, K Hirata, Y Kobayashi *Radiat. Phys. Chem.* **58** 525 (2000)
78. L Xie, D W Gidley, H A Hristov, A F Yee *J. Polym. Sci., Part B: Polym. Phys.* **33** 77 (1995)
79. Q Deng, Y C Jean *Macromolecules* **26** 30 (1993)
80. H F Szocs, O Sausa, K Kristiakova, J Kristiak, M Klimova *Eur. Polym. J.* **31** 1019 (1995)
81. J M Schmidt, F H J Maurer *Macromolecules* **33** 3879 (2000)
82. E-A McGonigle, J J Liggat, R A Pethrick, S D Jenkins, J H Daly, D Hayward *Polymer* **42** 2413 (2001)
83. G Dlubek, T Lüpke, H M Fretwell, M A Alam, A Wutzler, H-J Radusch *Acta Polym.* **49** 2326 (1998)
84. A A Askadskii, S A Tishin, V V Kazantseva, O V Kovriga *Vysokomol. Soedin., Ser. A* **32** 2437 (1990) [b]
85. K Okamoto, K Tanaka, N Katsube, O Sueoka, Y Ito, in *Proceedings of the 9th International Conference on Positron Annihilation. ICPA-9, Hungary, 1991* D-100
86. V P Shantarovich, T Suzuki, C He, V W Gustov *Radiat. Phys. Chem.* **67** 15 (2003)
87. Y Hirayama, T Yoshinaga, Y Kusuki, K Ninomiya, T Sakakibara, T Tamari *J. Membr. Sci.* **111** 169 (1996)
88. I B Kevdina, Yu M Sivergin, V P Shantarovich *Khim. Vys. Energ.* **30** 145 (1996) [c]
89. Y Wang, P T Inglefield, A J Jones *Polymer* **43** 1867 (2002)
90. A P M Kentgens, H A van Boxtel, R J Verweel, W S Veeman *Macromolecules* **24** 3712 (1991)
91. G J Kennedy *Polym. Bull.* **23** 605 (1990)
92. D R Morgan, E O Stejskal, A L Andrady *Macromolecules* **32** 1897 (1999)
93. M Mansfeld, W S Veeman *Chem. Phys. Lett.* **213** 153 (1993)
94. S K Brownstein, J E L Roovers, D Worsfold *Magn. Reson. Chem.* **26** 392 (1988)
95. T Suzuki, H Yoshimizu, Y Tsujita *Desalination* **148** 359 (2002)
96. T T P Cheung, P J Chu *J. Phys. Chem.* **96** 9551 (1992)
97. T R Stengle, K L Williamson *Macromolecules* **20** 1428 (1987)
98. J Demarquay, J Fraissard *J. Chem. Phys. Lett.* **136** 314 (1987)
99. J Fraissard, T Ito *Zeolites* **8** 350 (1988)
100. D W Breck *Zeolite Molecular Sieves* (New York: Wiley, 1974)
101. G Golemme, J B Nagy, A Fonseca, C Algieri, Yu Yampolskii *Polymer* **44** 5039 (2003)
102. V I Bondar, B D Freeman, Yu P Yampolskii *Macromolecules* **32** 6163 (1999)
103. Yu P Yampolskii, V G Berezkin, T P Popova, A P Korikov, B D Freeman, V I Bondar, T C Merkel *Polym. Sci., Ser. A* **42** 1023 (2000) [b]
104. T C Merkel, L G Toy, A L Andrady, H Gracz, E O Stejskal *Macromolecules* **36** 353 (2003)
105. M B Davydova, Yu P Yampolskii *Vysokomol. Soedin., Ser. A* **33** 574 (1991) [b]
106. G Golemme, J B Nagy, A Fonseca, C Algieri, in *Euromembrane 2000 (Abstracts of Papers), Maale Hachamisha, Israel, 2000* p. 312
107. T Suzuki, M Miyauchi, M Takegawa, H Yoshimizu, Y Tsujita, T Kinoshita *Macromolecules* **34** 3805 (2001)
108. J H Simpson, W Wen, A A Jones, J T Bendler *Macromolecules* **29** 2138 (1996)
109. B D Malhotra, R A Pethrik *Macromolecules* **16** 1175 (1983)
110. *Entsiklopediya Polimerov* (Encyclopaedia of Polymers) (Moscow: Sovetskaya Entsiklopediya, 1972)
111. D Hofmann, M Entrialgo-Castano, A Lerbret, M Heuchel, Yu Yampolskii *Macromolecules* **36** 8528 (2003)
112. V V Teplyakov, Doctoral Thesis in Chemical Sciences, Institute of Petrochemical Synthesis, Russian Academy of Sciences, Moscow, 1991
113. M S Syamala, R J Cross, M Saunders *J. Am. Chem. Soc.* **124** 6216 (2002)
114. M Saunders, H A Jimenez-Vasquez, J Cross, S Mroczkowski, M L Gross, D E Giblin, P J Poreda *J. Am. Chem. Soc.* **116** 2193 (1994)
115. J M Braun, J E Guillet *Adv. Polym. Sci.* **21** 107 (1976)
116. A E Nesterov, Yu S Lipatov *Obrashchennaya Gazovaya Khromatografiya v Termodinamike Polimerov* (Inverse Gas Chromatography in Thermodynamics of Polymers) (Kiev: Naukova Dumka, 1976)
117. M Kawakami, S Kagawa *Bull. Chem. Soc. Jpn.* **51** 75 (1978)
118. D R Stull, E F Westrum, G C Sinke *The Chemical Thermodynamics of Organic Compounds* (New York: Wiley, 1969)
119. K C B Dangayach, D C Bonner *Polym. Eng. Sci.* **20** 59 (1980)
120. Yu P Yampolskii, N E Kaliuzhnyi, S G Durgaryan *Macromolecules* **19** 846 (1986)
121. A Yu Alentiev, V P Shantarovich, T C Merkel, V I Bondar, B D Freeman, Yu P Yampolskii *Macromolecules* **35** 9513 (2002)
122. Yu Yampolskii, S Durgaryan, in *Chromatography and Thermodynamics. Determination of Physicochemical Parameters* (Warsaw: Institute of Physical Chemistry, Polish Academy of Sciences, 1986) p. 185
123. D W Van Krevelen *Properties of Polymers: Their Correlation with Chemical Structure* (3rd Ed.) (Amsterdam: Elsevier, 1990)

124. *Gas Encycopaedia. L'Air Liquide* (Amsterdam: Elsevier, 1976)
125. R C Reid, T K Sherwood *The Properties of Gases and Liquids* (New York: McGraw-Hill, 1966)
126. Yu P Yampolskii, S A Soloviev, M L Gringolts *Polymer* **45** 6945 (2004)
127. C S Paik, H Morawetz *Macromolecules* **5** 171 (1972)
128. J G Victor, J M Torkelson *Macromolecules* **20** 2241 (1987)
129. J S Royal, J G Victor, J M Torkelson *Macromolecules* **25** 729 (1992)
130. J S Royal, J M Torkelson *Macromolecules* **25** 4792 (1992)
131. A M Vasserman, A L Kovarskii *Spinovye Zondy i Metki v Fizicheskoi Khimii Polimerov* (Spin Probes and Labels in Physical the Chemistry of Polymers) (Moscow: Nauka, 1986)
132. Yu P Yampolskii, A M Vasserman, A L Kovarskii, S G Durgar'yan, N S Nametkin *Dokl. Akad. Nauk SSSR* **249** 150 (1979) [d]
133. Yu P Yampolskii, M V Motyakin, A M Wasserman, T Masuda, M Teraguchi, V S Khotimskii, B D Freeman *Polymer* **40** 1745 (1999)
134. A Kh Vorobiev, V S Gurman, T A Klimenko *Phys. Chem. Chem. Phys.* **2** 379 (2000)
135. S V Paschenko, S A Dzuba, A Kh Vorobiev, Yu V Toropov, Yu D Tsvetkov *J. Chem. Phys.* **110** 8150 (1999)
136. F P Chernyakovskii *Usp. Khim.* **48** 563 (1979) [*Russ. Chem. Rev.* **48** 306 (1979)]
137. A I Kornilov, A N Shchapov, E F Oleinik, N L Murav'eva, F P Chernyakovskii *Dokl. Akad. Nauk SSSR* **260** 124 (1981) [d]
138. N I Murav'eva, F P Chernyakovskii, Yu P Yampolskii, S G Durgar'yan *Zh. Fiz. Khim.* **61** 1894 (1987) [e]
139. Yu P Yampolskii, V P Shantarovich, F P Chernyakovskii, A I Kornilov, N A Plate *J. Appl. Polym. Sci.* **47** 85 (1993)
140. A A Stolov, D I Kamalova, A B Remizov, O E Zgadzai *Polymer* **37** 3049 (1996)
141. A A Stolov, D I Kamalova, A B Remizov *Polymer* **39** 5711 (1998)
142. D I Kamalova, A A Stolov, S A Petrova, A B Remizov *Zh. Fiz. Khim.* **74** 1997 (2000) [e]
143. S A Petrova, Candidate Thesis in Chemical Sciences, Kazan State Technological University, Kazan, 2002
144. M L Greenfield, D N Theodorou *Macromolecules* **26** 5461 (1993)
145. V M Shah, S A Stern, P J Ludovice *Macromolecules* **22** 4660 (1989)
146. S Neyertz, D Brown *J. Chem. Phys.* **115** 708 (2001)
147. S Trohalaki, C C De Bolt, J E Mark, H L Frisch *Macromolecules* **23** 813 (1990)
148. I A Ronova, E M Rozhkov, A Yu Alentiev, Yu P Yampolskii *Macromol. Theory Simul.* **12** 425 (2003)
149. S Misra, W L Mattice *Macromolecules* **26** 7274 (1993)
150. S Niemela, J Leppanen, F Sundholm *Polymer* **37** 4155 (1996)
151. R Voorinntholt, M T Kosters, G Vegter, G Vriend, W G J Hol *J. Mol. Graphics Modell.* **7** 243 (1989)
152. T Zheng, J R Fried *Sep. Sci. Technol.* **36** 959 (2001)
153. D Hofmann, L Fritz, J Ulbrich, C Schepers, M Böhning *Macromol. Theory Simul.* **9** 293 (2000)
154. H Sun *J. Phys. Chem. B* **102** 7338 (1998)
155. D N Theodorou, U W Suter *Macromolecules* **18** 1467 (1985)
156. D N Theodorou, U W Suter *Macromolecules* **19** 139 (1986)
157. D Hofmann, M Heuchel, Yu Yampolskii, V Khotimskii *Macromolecules* **35** 2129 (2002)
158. V E Raptis, I G Economou, D N Theodorou, J Petrou, J H Petropoulos *Macromolecules* **37** 1102 (2004)
159. V S Khotimskii, V G Filippova, I S Bryantseva, V I Bondar, V P Shantarovich, Yu P Yampolskii *J. Appl. Polym. Sci.* **78** 1612 (2000)
160. Y Ichiraku, S A Stern, T Nakagawa *J. Membr. Sci.* **34** 5 (1987)
161. R Srinivasan, S R Auvil, P M Burban *J. Membr. Sci.* **86** 67 (1994)
162. I Pinnau, L G Toy *J. Membr. Sci.* **116** 199 (1996)
163. T C Merkel, V Bondar, K Nagai, B D Freeman *J. Polym. Sci., Part B: Polym. Phys.* **38** 273 (2000)
164. E Schmidtke, K Günter-Schade, D Hofmann, F Faupel *J. Mol. Graphics Modell.* **22** 309 (2004)
165. C Nagel, E Schmidtke, K Günter-Schade, D Hofmann, D Fritsch, T Strunkus, F Faupel *Macromolecules* **33** 2242 (2000)
166. K Ciesielski, A L Dawidowicz, T Goworek, B Jasinska, B Wawryszczuk *J. Chem. Phys. Lett.* **289** 41 (1998)
167. H Schmitz, F Müller-Plathe *J. Chem. Phys.* **112** 1040 (2000)
168. M Heuchel, D Hofmann, P Pullumbi *Macromolecules* **37** 201 (2004)
169. X Y Wang, K M Lee, Y Lu, M T Stone, I C Sanchez, B D Freeman *Polymer* **45** 3907 (2004)
170. X Y Wang, P J Veld, Y Lu, I C Sanchez, B D Freeman, I C Sanchez *Polymer* **46** 9155 (2005)
171. H F M Mohamed, N S Abd El-Aziz *Polymer* **42** 8013 (2001)
172. D Hofmann, L Fritz, J Ulbricht, D Paul *Comput. Theor. Polym. Sci.* **10** 419 (2000)
173. L Fritz, D Hofmann *Polymer* **38** 1035 (1997)
174. D Hofmann, L Fritz, J Ulbricht, D Paul *Polymer* **38** 6145 (1997)
175. E Tocci, D Hofmann, D Paul, N Russo, E Drioli *Polymer* **42** 521 (2001)

[a] — *Chem. Phys. Rep. (Engl. Transl.)*
[b] — *Polym. Sci. (Engl. Transl.)*
[c] — *High Energy Chem. (Engl. Transl.)*
[d] — *Dokl. Phys. Chem. (Engl. Transl.)*
[e] — *Russ. J. Phys. Chem. (Engl. Transl.)*